

# Understanding the functions of carbon in the negative active-mass of the lead–acid battery: A review of progress



Patrick T. Moseley<sup>a,\*</sup>, David A.J. Rand<sup>b</sup>, Alistair Davidson<sup>c</sup>, Boris Monahov<sup>d</sup>

<sup>a</sup> Ivy Cottage, Chilton, OX110RT, United Kingdom

<sup>b</sup> CSIRO Energy, Melbourne, Victoria, 3169, Australia

<sup>c</sup> International Lead Association, London, United Kingdom

<sup>d</sup> Advanced Lead-Acid Battery Consortium, Durham, NC, USA

## ARTICLE INFO

### Keywords:

Capacitance  
Extra-carbon effect  
Functional group  
Hydrogen evolution  
Metal additives  
Physical effects

## ABSTRACT

The addition of supplementary carbon to lead–acid batteries that are intended for use in emerging automotive duties can provide improvement in two aspects of performance.

(i) In both hybrid electric and battery electric vehicles that are designed to preserve energy through the operation of regenerative-braking, conventional lead–acid batteries exhibit a rapid decline in the efficiency of the recuperative charging (which can involve rates up to 30C<sub>7</sub>) and fail quickly as a result of an accumulation of lead sulfate on the negative plate. It has been widely reported that supplementary carbon — either intimately mixed with the negative active-material or included as a separate component attached to the plate — can enhance charge-acceptance.

(ii) Full-hybrid electric and battery electric vehicles employ high-voltage batteries composed of large numbers of cells connected in series. Consequently, when conventional lead–acid batteries are used in such configurations, the continuous cycling encountered in normal driving will almost certainly lead to divergence in the states-of-charge of the unit cells and thereby demand periodic equalization charges. In this application, it has been demonstrated that lead–acid batteries with supplementary carbon incorporated into the negative plate are rendered immune to the divergence problem and therefore operate without the need for an equalization charge.

The inclusion of supplementary carbon does, however, promote hydrogen evolution and failure due to the loss of water from the electrolyte solution. Current research efforts are directed towards methods by which this disadvantage can be mitigated without losing the benefits that the addition of carbon provides.

This review covers the extensive research that has been conducted to understand the mechanism by which the additional carbon operates, the additional studies that have sought to identify the best types and optimum amounts of carbon that should be used, together with the most effective manner for their deployment.

## 1. Recognition of extra carbon as a boost to dynamic charge-efficiency

For decades, negative plates in lead–acid batteries have been provided with a combination of carbon, barium sulfate and an organic additive, which is usually a wood extract, e.g., a lignosulfonate. These additives are collectively called an ‘expander’, although this term is often used purely for the organic component of the mix. During charge–discharge cycling, the expander serves to prevent individual crystals of lead from growing and combining into a dense structure with a low surface-area and, therefore, a low electrical capacity. The total amount of expander used in industrial valve-regulated lead–acid (VRLA)

batteries varies between 1.0 and 2.5 wt.% with respect to the weight of the oxide in the paste mix. The individual additions of carbon, barium sulfate and organic material vary according to the manufacturer’s specifications [1].

The benefits of including additional carbon in the negative active-mass beyond the level that is normal for the ‘expander’ function were first demonstrated by the work of Nakamura and Shiomi [2,3], who made negative plates that contained up to ten times the customary level of carbon. The actual amounts were not disclosed but, based on typical practice, were believed to be about 2.0 wt.% of the negative active-material loading. The trials, which were directed towards both electric vehicle and photovoltaic (PV) power applications, were conducted with

\* Corresponding author.

E-mail addresses: [moseley@ila-lead.org](mailto:moseley@ila-lead.org) (P.T. Moseley), [David.Rand@csiro.au](mailto:David.Rand@csiro.au) (D.A.J. Rand), [Davidson@ila-lead.org](mailto:Davidson@ila-lead.org) (A. Davidson), [Monahov@ila-lead.org](mailto:Monahov@ila-lead.org) (B. Monahov).

<https://doi.org/10.1016/j.est.2018.08.003>

Received 3 July 2018; Received in revised form 2 August 2018; Accepted 2 August 2018

Available online 22 August 2018

2352-152X/ © 2018 The Authors. Published by Elsevier Ltd. This is an open access article under the CC BY-NC-ND license (<http://creativecommons.org/licenses/by-nc-nd/4.0/>).

**Nomenclature***Acronyms and initialisms used in the text*

1BS	Monobasic lead sulfate (PbO·PbSO <sub>4</sub> )
3BS	Tribasic lead sulfate (3PbO·PbSO <sub>4</sub> ·H <sub>2</sub> O)
4B3	Tetrabasic lead sulfate (4PbO·PbSO <sub>4</sub> )
a.c.	Alternating current
AC	Activated carbon
AGM	Absorptive glass mat
ALABC	Advanced Lead–Acid Battery Consortium
BET	Brunauer–Emmett–Teller (technique for measuring specific surface-area)
BM	Ball mill
BP	Barton pot
BMS	Battery management system
BSS	Battery support system
CB	Carbon black
CSIRO	Commonwealth Scientific and Industrial Research Organisation
d.c.	Direct current
DCA	Dynamic charge-acceptance
DCE	Dynamic charge-efficiency
EAC	Electrochemically active carbon
EES	Electrical energy storage
EF	Fermi level
EG	Expanded graphite
FG	Flake graphite
GO	Graphene oxide
HER	Hydrogen evolution reaction
HEV	Hybrid electric vehicle
HRPSoC	High-rate partial-state-of-charge
LD	Donor level
OAN	Oil Absorption Number
PSoC	Partial state-of-charge
S	Siemens (= A V <sup>-1</sup> or Ω <sup>-1</sup> )
SoC	State-of-charge
SoCOT	Operational state-of-charge
VRLA	Valve-regulated lead–acid (battery)
XPS	X-ray photoelectron spectroscopy

*Roman letters*

A	Ampere; also real electrode surface-area (in m <sup>2</sup> )
Å	Angstrom (10 <sup>-10</sup> m)
AC	Activated carbon
Ah	Ampere-hour
c	Molar concentration (mol L <sup>-1</sup> )
cm	Centimetre
°C	Degree Celsius
C	Coulomb (= 1 A s)
C	Capacitance (in F = A s V <sup>-1</sup> )
C <sub>s</sub>	Specific-area capacitance (F cm <sup>-2</sup> )
C <sub>m</sub>	Specific capacitance (F g <sup>-1</sup> )
C <sub>diff</sub>	Ionic diffuse-layer capacitance (F)
C <sub>H</sub>	Helmholtz double-layer capacitance (F)
C <sub>sc</sub>	Space charge capacitance (F)
C <sub>x</sub> /t	Discharge rate (X = hour rate; t = specified discharge

d	Thickness of double-layer (m)
e	Mathematical constant = 2.71828
e <sup>-</sup>	Electron (negative charge: 1.602 × 10 <sup>-19</sup> C; mass: 9.109 × 10 <sup>-31</sup> kg)
E <sub>F</sub>	Fermi level energy
E <sub>V</sub>	Energy of the valence band
E <sub>C</sub>	Energy of the conduction band
F	Farad (= C V <sup>-1</sup> )
F	Faraday constant (= 96 485 C mol <sup>-1</sup> )
g	Gram
i <sub>o</sub>	Exchange-current density (A cm <sup>-2</sup> )
I	Current (A)
I <sub>bat</sub>	Current (A) through the parallel connection of a capacitor and a charge-transfer component (a Faradaic element)
I <sub>C</sub>	Current (A) through a capacitor
I <sub>CT</sub>	Current (A) through a charge-transfer component (a Faradaic element)
J	Joule (1 J = 1 W s)
k	Kilo (10 <sup>3</sup> )
km	Kilometer
kW	Kilowatt
kWh	Kilowatt–hour
K	Kelvin (a measure of absolute temperature)
m	Metre; also milli (10 <sup>-3</sup> )
mg	Milligram
min	Minute
ms	Millisecond
m	Mass (kg)
pm	Picometre (10 <sup>-12</sup> m)
Q	Electric charge (in C = 1 A s)
R	Ohmic resistance (in ←Ω), real part of impedance
R <sub>CT</sub>	Resistance (in Ω) of a charge-transfer component (a Faradaic element)
R	Universal gas constant (8.3145 J mole <sup>-1</sup> K <sup>-1</sup> )
s	Second
S	Surface-area (m <sup>2</sup> )
T	Absolute temperature (K)
U	Volt (V); symbol commonly used in German forums; SI symbol is V
V	Voltage; also volume (m <sup>3</sup> )
W	Watt (1 W = 1 J s <sup>-1</sup> )
Wh	Watt–hour
wt.%	Percentage by weight

*Greek letters*

ε <sub>0</sub>	Permittivity of vacuum (98.854 × 10 <sup>-12</sup> F m <sup>-1</sup> )
ε <sub>r</sub>	Relative permittivity of the dielectric
μ	Micro (10 <sup>-6</sup> )
ρ	Density (kg m <sup>-3</sup> )
τ	Time constant (s), τ = RC
φ <sub>m</sub>	Work function
φ <sub>B0</sub>	Schottky barrier height
χ	Electron affinity
Ω	Ohms

AGM-VRLA batteries that operated under PSoC conditions to lessen overcharge effects. Batteries with standard levels of carbon failed quickly due to the build-up of lead sulfate in the negative plate. By contrast, the companion positive plate was fully-charged. Batteries with extra carbon enjoyed appreciably longer operating lives. Recently, it

has been reported [4] that the additional carbon results not only in an increased cycle-life but also in greater specific energy at high rates.

To date, the prime aim of the work on carbon addition has been to support 12-V automotive batteries in micro-HEVS with regenerative-braking where the shortcomings of ‘dynamic charge-acceptance’ (DCA)

have emerged. The DCA is quantified as the average charging current (or charge integral) over either one or all recuperation pulses of a representative PSOC micro-cycling sequence, and can be normalized to the battery's nominal capacity, i.e.,  $A\text{ h}^{-1}$ . In practice, however, DCA represents the charge that is accepted by both the reduction of lead sulfate to lead and the evolution of hydrogen. Nevertheless, since it is primarily the former reaction that should be encouraged, it is the 'dynamic charge-efficiency' (DCE), which represents only the  $\text{PbSO}_4 | \text{Pb}$  reaction, that should be the focus of attention and quoted in terms of only those amperes (A) accepted into the lead sulfate reduction per ampere-hour (Ah) of battery capacity.

Developments [5] have revealed that extra carbon enhances charge efficiency under the high-rate charging conditions that occur during the 'stop-start' duty of micro-HEVs. Studies conducted on higher voltage lead-acid batteries for medium- and full-HEVs found that the states-of-charge of series-connected cells with additional carbon in their negative active-mass remained balanced and therefore periodic equalization was not required.

Several modes of deployment of the supplementary carbon have been shown to be effective in producing the beneficial effects outlined above [6]. Carbon can be intimately mixed with the negative active-material during plate manufacture. Alternatively, the structural component of the plate – the grid – can either be fabricated of carbon on to which a conventional negative paste mix can be applied, or a conventional negative plate can be sandwiched between sheaths of carbon, as in the design of the UltraBattery™ [6].

Although the advantages have been demonstrated, an unequivocal determination of the means by which carbon assists the recharge of lead-acid is a subject of continuing study. Such knowledge will provide a deeper appreciation of the functional relationship between product and required duty, which is essential for the future development and design of cells for new and emerging applications of lead-acid technology. Candidate mechanisms for the 'extra-carbon effect' are discussed in the following Section 2.

## 2. Understanding the 'extra-carbon effect'

Various empirical studies have provided evidence that the addition of certain forms of carbon can invest the negative plate with improved charge-acceptance. The optimum amount of extra carbon has been found to be around 2 wt.% of the negative active-material. The incorporation of greater amounts of carbon renders the paste mix difficult to handle. Further, it has become clear that the more the amount of carbon added, the greater is the surface-area which is contributing to hydrogen evolution. Consequently, there is a down-turn in performance at high carbon loadings [7]; see Section 3.

In recent years, there has been much discussion over the mechanism by which the carbon component can enhance negative-plate performance. The effectiveness of any particular form of carbon in this role is likely to be influenced by a number of properties that include:

- the presence of metal contaminants at the carbon surface;
- surface functional groups;
- hydrogen evolution overpotential;
- electronic conductivity;
- capacitance;
- the size of any pores in the carbon;
- the affinity of the carbon for lead;
- interaction with the organic component of the expander mix;
- wettability by the aqueous electrolyte solution;
- specific surface-area ( $\text{cm}^2\text{ g}^{-1}$ )

The challenge of the optimization process is to identify those properties that are the most important and this can only be achieved through a full understanding of the respective mechanism(s) by which the properties exert an influence. As many as eight different functions

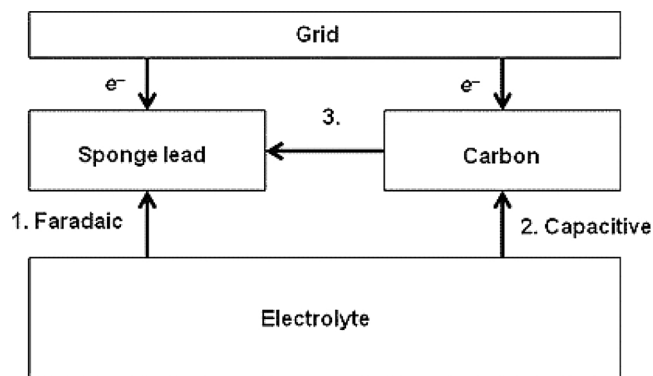


Fig. 1. Schematic of current fluxes during and after a short charge event on a negative plate that contains carbon [6].

have been put forward [8]. Nonetheless, the growing body of evidence points to just three principal mechanisms that are each likely to have a significant beneficial influence on the function of the negative plate during PSOC operation, as well as on the performance of cells in long series-connected strings. The overall situation remains complicated, however, because the operative mechanism is determined by the specific duty that the battery is performing. Each of these actions of carbon is considered in more detail, as follows.

### 2.1. Capacitance: current flows during and after a charge event

In the first case, the carbon serves as a capacitive buffer to absorb charge current at higher rates than can be accommodated by the Faradaic (i.e., electrochemical) reaction; see Fig. 1 [6]. A conventional negative electrode will itself have an attendant double-layer but the capacitive function (capacitance of the negative is normally in the range  $0.06\text{--}0.08\text{ F g}^{-1}$  [9]) only becomes noticeable when the surface-area is magnified appreciably by the addition of an appropriate form of carbon. It has been reported [10] that the double-layer capacitance of the negative active-mass exhibits a linear correlation with the external surface-area of the carbon that is added.

When a charge event applied to a lead-acid cell is discontinued, although the external current is zero the double-layer remains charged and this results in a local current between the components of the negative active-material [11]. The current is caused by the discharging of the double-layer via the Faradaic reaction and thereby the electrode potential changes to its equilibrium value with a characteristic time constant. The amount of charge involved can be substantial if the surface-area of conducting material is augmented by the inclusion of an appropriate form of carbon. The time constant,  $\tau$ , for the equilibration

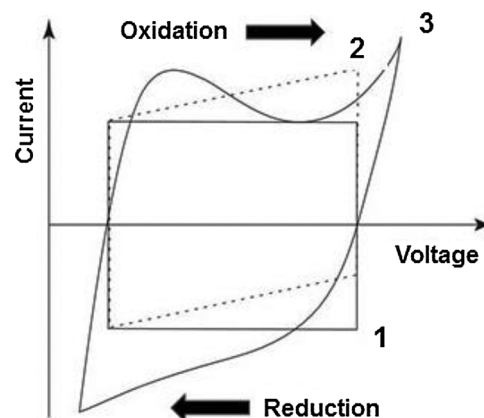


Fig. 2. Cyclic voltammograms: 1 ideal capacitor; 2 capacitor with internal resistance; 3 carbon supercapacitor with pseudocapacitance.

**Box 1**

Time constant of a capacitor.

During charging, the time constant is the time taken (base unit, seconds) for the voltage across a capacitor to increase by 63.2% of the difference between its present and final values. This value is derived from the mathematical constant  $e$ , specifically:  $1 - e^{-1}$  ( $e = 2.71828$ ).

During discharging, the voltage will fall by 63.2%–36.8% of its maximum value in one time constant period.

Charge or discharge of a capacitor will be virtually complete after 5 times the time constant.

process (see [Box 1](#)) is estimated by equating the double-layer discharge current to the charging current that is going into the Faradaic reaction and can be approximated [12] as:

$$\tau = RTC_s / Fi_o \quad (1)$$

Where:  $R$  is the universal gas constant ( $8.3145 \text{ J mole}^{-1} \text{ K}^{-1}$ );  $T$  is the absolute temperature (K);  $C_s$  is the specific-area capacitance ( $\text{F cm}^{-2}$ );  $F$  is the Faraday constant ( $96485 \text{ A s mol}^{-1}$ );  $i_o$  is the exchange-current density ( $\text{A cm}^{-2}$ ).

Reactions that proceed relatively quickly have a small time constant, whereas those that are kinetically sluggish result in a large time constant. By way of example [12], the zinc electrode has rapid kinetics with an exchange-current of around  $10^{-2} \text{ A cm}^{-2}$  that gives rise to a time constant of the order of  $50 \mu\text{s}$ . The nickel hydroxide electrode has a time constant of around 5 ms. Since both these time constants are so short, the involvement of the equilibration process outlined above has been largely ignored for both the zinc and the nickel electrode systems. By contrast, the kinetics of the electrode reactions in a lead–acid cell are much slower, namely:  $4 \times 10^{-7} \text{ A cm}^{-2}$  at the positive plate, and  $4.96 \times 10^{-6} \text{ A cm}^{-2}$  at the negative. With an augmented carbon inventory, the negative plate can contribute a specific-area capacitance of up to  $30 \mu\text{F cm}^{-2}$  whereby the time constant can be of the order of seconds and the charge equilibration (flux 3 in [Fig. 1](#)) can be regarded as a significant process that follows the removal of the external charging voltage. Under HRPSoc conditions, charge from external events, such as regenerative-braking in vehicle applications, is taken up by the double-layer and thus boosts DCE. When the external input is discontinued, this charge is re-equilibrated between the double-layer and the Faradaic reaction.

Recently, it has been shown [13] that cyclic voltammetry can be used to quantify the capacitive contribution to the charge-acceptance. A description of cyclic voltammetry and its value as an experiment technique is outlined in [Box 2](#), below.

The three regions of a cyclic voltammogram that arise, respectively, from the Faradaic deposition of lead, the capacitive charging and the Faradaic evolution of hydrogen are illustrated in [Fig. 3](#) [13]. The relative location of these regions is significant. The area that represents hydrogen evolution has moved to the right (i.e., to a less negative potential) due to the addition of carbon. Simultaneously, the current

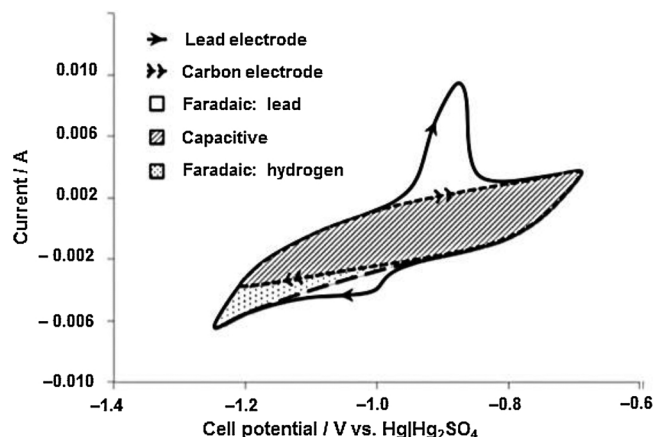


**Fig. 3.** Identification of contributions from lead deposition (Faradaic), double-layer adsorption/desorption (capacitive) and hydrogen evolution (Faradaic) to cyclic voltammograms for lead and carbon electrodes (carbon black, acetylene black, graphite) [13].

flowing into the capacitance at all values of potential has expanded. To take advantage of this latter feature without invoking an increase in water electrolysis, it is necessary with a flooded cell to limit the potential or the duration of charge events, and with a valve-regulated cell to depend on the efficient operation of the oxygen-recombination cycle (even at low states-of-charge). Although the introduction of extra carbon may reduce the overpotential of hydrogen evolution, it is possible for cells thus-treated to provide a long operational life without excessive loss of water provided that the charge events to which they are exposed are limited in duration or potential.

The relative amounts of charge to the abovementioned three reactions on three different forms of carbon are compared with those on a bare lead electrode in [Fig. 4](#) [13]. All three carbons provide significantly higher charge capacity than the lead-only electrode. The charge capacity of lead electrodeposition for carbon black, acetylene black, graphite and lead during the reduction cycle is 8.9, 3.5, 6.9 and 2.3 mC, respectively. The charge capacity of the carbon black (44.9 mC) is about double that of the acetylene black (22.6 mC). By comparison,

**Box 2**

Cyclic voltammetry — surveying the reactivity of materials.

This technique involves measuring the current response of an electrode to a linearly increasing and decreasing cycle of potential at a fixed scan rate. The voltammograms can provide information such as: (i) the potential at which oxidation and reduction processes occur, (ii) the oxidation state of the redox species, (iii) the number of electrons involved, (iv) the rate of electron transfer, (v) possible chemical processes associated with the electron transfer, (vi) adsorption effects, and (vii) characterization and measurement of capacitance.

An ideal capacitor exhibits a rectangular cyclic voltammogram (cf., [Fig. 2](#)), which describes a purely electrostatic mechanism of energy storage, in which the flowing current is independent of potential. Carbon electrodes, however, can deviate from this rectangular shape, and reveal reversible redox peaks that correspond to pseudo-Faradaic reactions; see [Box 3](#), Section 3.3 (v.i.).

The charge accumulated in the capacitor strongly depends on the electrode potential, and the observed distance and asymmetry between the oxidation and reduction peaks reflect kinetically inhibited and less-reversible electrode processes during charging and discharging the pseudocapacitance. The peak currents depend on structural anisotropy, the active area and the activation procedure of the material. For example, the double-layer pseudocapacitance of cleaved graphite basal and polished edge planes is 12–20 and 50–70  $\mu\text{F cm}^{-2}$ , respectively, whereas graphite powders have 20–35  $\mu\text{F cm}^{-2}$  and carbon blacks 4.5–10  $\mu\text{F cm}^{-2}$  (real surface-area).

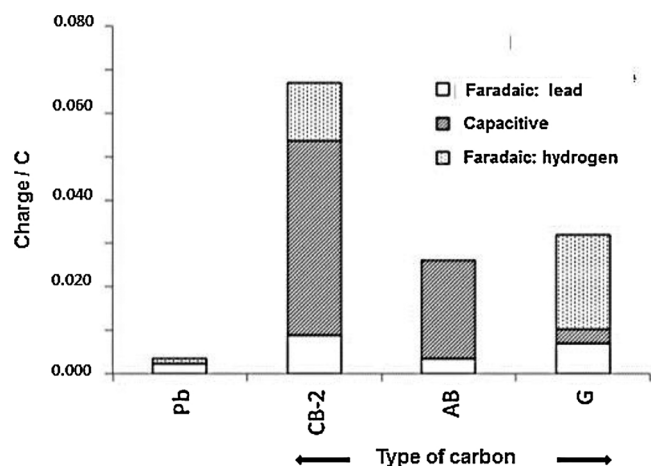


Fig. 4. Respective charge capacity (coulombs) for lead deposition, capacitance and hydrogen evolution for mixtures lead + carbon black (CB-2), lead + acetylene black (AB) and lead + graphite (G) compared with that for a bare lead electrode (Pb) [13].

the graphite powder does not display any capacitive behaviour due to its much lower surface-area but it does have notable gassing characteristics.

## 2.2. Assisting electrochemistry by extending the conducting surface-area

The second effect of carbon is to extend the area of the electrode microstructure on which electrochemical charge and discharge reactions can take place. During the charge reaction, lead can be deposited on the additional surface, as seen in Fig. 5 [14].

Cycle tests under HRPSoc conditions of cells that contain extra carbon have provided strong evidence [15] that the electrochemical and chemical processes can take place not only on the surface of lead metal, but also on the surface of carbon; see Fig. 6. Subsequent research [16] has confirmed that two electrical systems are operating on carbon at the negative plate, namely:

- the capacitive system, which involves high-rate charging and discharging of the electric double-layer (the mechanism that is described in Section 2.1, above);
- the conventional lead electrochemical system, which comprises the oxidation of lead to lead sulfate during discharge and the reverse process during charge

Significantly, it has been observed [16] that the dominating process in the electrode reaction is the double-layer capacitance (non-Faradaic

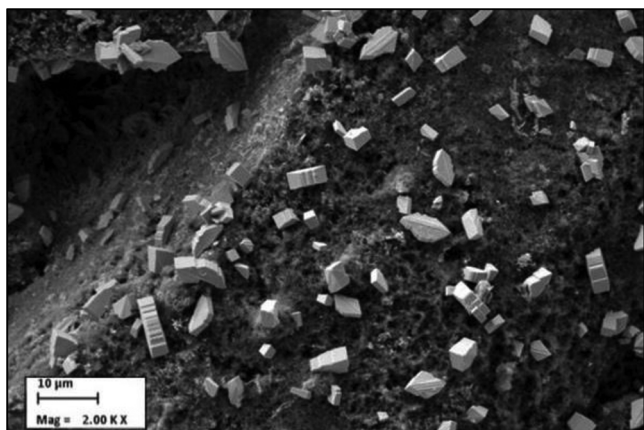


Fig. 5. Lead crystals electrodeposited on a carbon surface [14].

process) when the charge and the discharge cycles are limited to 5 s of duration. If, however, the charge and the discharge durations are between 30 and 50 s, then the dominant reactions are the Faradaic processes related to lead sulfate dissolution or lead deposition. These observations are consistent with the above calculation of the time constant for the transfer of charge between the two component materials of the negative electrode. A duty cycle that is completed in a few seconds is accommodated by the first (capacitive) mechanism, while longer periods of discharge and charge require the involvement of the Faradaic reaction.

## 2.3. Physical effects

The third way in which carbon can modify the behaviour of the negative active-material is by means of physical effects, for instance by obstructing the growth of lead sulfate crystals, by maintaining channels for irrigation of the electrode by the electrolyte solution, or by restricting tendency to acid stratification in flooded batteries. In all such cases, there is no need for the carbon to be in a conductive form. The supporting evidence for the three physical effects is as follows.

### 2.3.1. Steric hindrance

Studies have indicated [17,18] that the carbon added to the negative active-mass can act as a steric hindrance to the crystallization of lead sulfate and thus helps to maintain a high surface-area for the discharge product. By obstructing the growth of lead sulfate crystals that occurs via ‘Ostwald Ripening’, the carbon ensures that the recharge of lead sulfate back to lead is able to continue. In support of this theory, it has been reported [19] that HRPSoc cycle-life is enhanced when titanium dioxide (a poorer electronic conductor), rather than graphite, is used as the additive. Consequently, whereas cycle-life is improved by using either titanium dioxide or graphite (to different extents), the effect of the latter is not necessarily due to its conductivity alone.

Longer cycle-lives under HRPSoc duty have been achieved with carbon of larger particle-size (i.e., micron-size rather than nanometre) [19]. This information has given rise to the view [5] that small particles of carbon can become progressively buried within crystals of lead sulfate and accordingly their effectiveness is lost.

Other investigators [16] have reported that some activated carbon additives can *reduce* the pore structure of the negative electrode — thus apparently conflicting with the work of other researchers [20,21]. One consequence of a reduction in pore size is that the access of  $\text{SO}_4^{2-}$  ions to the innermost pores is impeded. On the other hand,  $\text{H}^+$  ions may still diffuse out of the pores and allow the pH to rise locally to a value at which  $\alpha\text{-PbO}$  is formed. This phase, which is clearly visible in X-ray diffraction records, is deleterious to the continued function of the negative active-material because the formation of the oxide is irreversible.

### 2.3.2. Electrode irrigation

It has been advocated [19,20] that the addition of carbon increases the porosity of the negative electrode by providing an additional structural skeleton that facilitates diffusion of the electrolyte solution from the surface to the interior of the plate. As a result, sufficient sulfuric acid is supplied to keep pace with the electrode reaction during HRPSoc operation.

One other possible mechanism for electrode irrigation remains to be explored. A property of many high specific surface-area carbon materials is that they interact strongly, through specific adsorption, with many aqueous acid solutions. As a result, some carbons can give rise to electro-osmotic pumping effects, whereby the choice of an appropriate potential can cause a net flow of electrolyte solution in or out of the plate [22,23]. Such effects could actively assist the movement of sulfuric acid into the interior of the negative plate, thereby counteracting the adverse distribution of electrolyte solution. This, in turn, would act to reduce the initial uneven distribution of lead sulfate in the negative active-material and, later in service, would help to prevent preferential

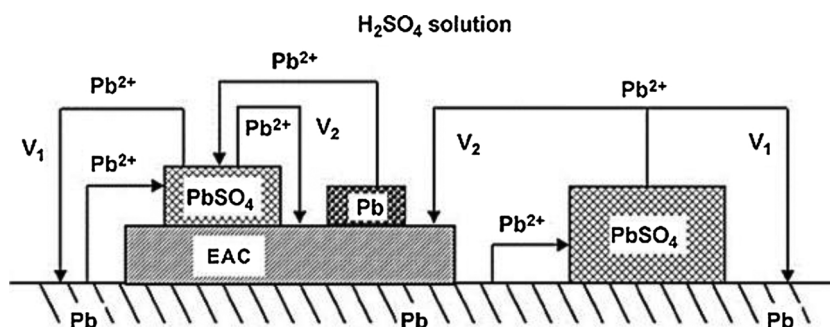


Fig. 6. Schematic illustration of how Faradaic reactions of the negative plate can take place on both lead and carbon surfaces. (EAC stands for electrochemically active carbon.) [15].

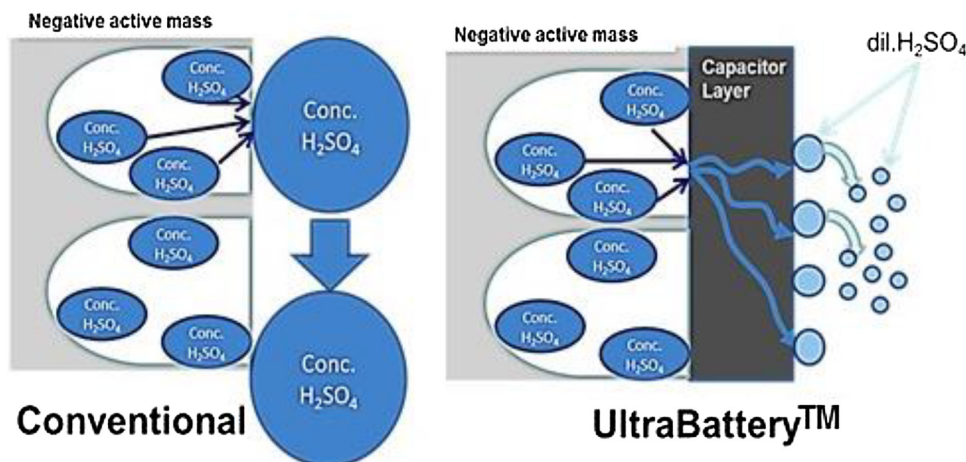


Fig. 7. Limitation of acid stratification in a flooded UltraBattery™ [24].

charging in the interior of the plate. To date, however, there does not appear to have been any observations of this effect during HRPSOC operation.

### 2.3.3. Restricting stratification

Flooded batteries that are subject to deep-discharge cycling may fail when the denser sulfuric acid that is produced during charging gravitates to the lower part of the cell. Battery designs with a carbon sheet adjacent to, and in contact with, the plate surface (as in the UltraBattery™) are able to restrict the stratification process and thereby extend life. The mechanism can be explained as follows. In general, the negative plate is comprised of comparatively large pores with an average diameter of about 1  $\mu\text{m}$ . During charging, the highly concentrated solution of sulfuric acid produced within the pores takes the form of large droplets that flow out from the negative plate, as illustrated in Fig. 7 [24]. The heavy and large droplets then settle quickly to the bottom of the cell and thereby give rise to stratification.

By contrast, the negative plate of the UltraBattery™ is covered with a capacitor layer that has pores of one order of magnitude smaller in average diameter than that of the lead–acid negative plate. Therefore, when the highly concentrated sulfuric acid produced within the lead–acid negative plate during the charging passes through the capacitor layer, it is broken down into many small droplets. Since small droplets will settle at a slower rate, there is sufficient time to diffuse and mix with surrounding electrolyte solution of lower relative density. Consequently, the stratification effect is restrained.

## 2.4. Summary of principal beneficial actions of extra carbon

Clearly, there are at least three ways by which the presence of carbon can modify the performance of the negative plate of a lead–acid battery, as follows.

- (i) The capacitive process is broadly favoured by carbon that has large surface-area and is in close proximity to the current-collector (grid). It is not necessary, however, for the carbon to be mixed intimately with the sponge lead component of the negative electrode.
- (ii) The surface-area effect also requires the carbon to be conductive and in contact with the current-collector. On the other hand, given that carbon promotes a bulk rather than a surface process, the surface-area can be less than that required to instigate the capacitive process.
- (iii) Carbon deployed to take advantage of the obstruction of crystal growth, does not have to be conducting, but it must be intimately mixed with the sponge lead and should not be very finely-divided or its efficacy will wane over time. In order to reduce the menace of acid stratification, carbon needs to be present as a porous sheet adjacent to the outer surface of the negative plate of a flooded cell.

In view of the conflicting requirements for the carbon to function in these several ways, it is not surprising that workers who are seeking to optimize the HRPSOC performance of lead–acid batteries have resorted to evaluating combinations of different types of carbon.

## 3. Limits to the amount of carbon that can be accommodated

### 3.1. Paste-mixing issues

The manufacture of pasted plates for lead–acid batteries involves a sequence of processing steps that successively impart the chemical and physical properties required for a premium product. Consequently, there is every expectation that conventional plate-making will have to be modified to accommodate extra carbon without its degradation and in an optimum dispersion within the negative active-material. The

addition of even small supplementary amounts (1–2 wt.%) of some forms of carbon can increase the specific surface-area of the overall negative active-material by an order of magnitude or more. In general, it is found that, in order to create a manageable paste mix, more water must be included than is used in the absence of extra carbon. The structure of the carbon particles is also important in this regard. Low surface-area carbons with a low Oil Absorption Number (OAN) may be dry-mixed but carbons with a high surface-area and a high OAN require large amounts of additional water to ensure satisfactory pasting [25]. The paste-mixing procedure exercises a large influence on the dispersion of the carbon and the performance of the negative active-material.

### 3.2. Hydrogen evolution

The addition of carbon to the negative active-mass can serve to augment the surface-area of the electrode substantially and in such cases it is common for there to be an increase in the hydrogen evolution rate (HER) during charging [26]. Aggravated HER leading to the dry-out of cells can become a serious failure mode.

In general an increase in the HER may arise from:

- (i) an increase in the applied potential;
- (ii) an increase in the surface-area of the active-material; as noted above, it has been suggested [7] that the HER correlates linearly with the external surface-area of the carbon;
- (iii) the presence of certain impurities.

Items (ii) and (iii) relate to a lowering of the hydrogen overpotential that may be brought about by the addition of extra carbon to the negative active-mass.

Key steps in the HER are the arrival and absorption of protons at the solid surface and the acquisition of an electron by each proton to form a neutral hydrogen atom. The adsorbed hydrogen atoms must collect in pairs before departing as gas molecules; see Fig. 8.

There are marked variations in hydrogen gassing behaviour between the different classes of carbon (e.g., graphite, carbon black, activated carbon). A recent study [26] has, as expected, shown that the presence of a significant concentration of iron invests graphite with a high level of hydrogen evolution. The work also reported that both graphites and carbon black materials have notably higher specific currents ( $A\ g^{-1}$ ) than activated carbon materials.

In another investigation [29], weight loss was monitored for cells that contained variously carbon black (CB), expanded graphite (EG) and flake graphite (FG). The weight loss and concomitant loss of capacity compliment the findings reported in reference [26]. It was found (Fig. 9) that the cell that contained flake graphite was particularly prone to weight loss and capacity degradation.

The degree of improvement in HRPSoc cycle-life that results from the deployment of supplementary carbon depends on the amount

added. The improvement in performance that can be achieved in this way reaches a peak at different concentrations for different carbons but in all cases that have been investigated, the maximum benefit is obtained for additions of between 0.5 and about 2 wt.%. For example, the data in Fig. 10 shows that the peak for a cell with an added activated carbon (unspecified) occurs at 1 wt.% [30].

The observed peak in cycle-life performance occurs for the following reason. As soon as any amount of carbon is added to the negative active-mass there are two results. First, the carbon is able to accommodate high-rate charge pulses through a capacitive function so that irreversible sulfation is precluded, and second, hydrogen evolution is aggravated. For small additions of carbon (up to the point that corresponds to the peak in cycle-life), the benefit of avoiding sulfation is greater than the deleterious effect of increased hydrogen evolution. After sufficient carbon has been added to overcome the danger of sulfation when the duty involves the high-rate charge events, the further addition of the additive will serve only to increase hydrogen evolution with no accompanying advantage. If the HER could be avoided, then the favourable action of carbon could probably be extended so that a greater fraction of the energy that is available in high-rate charge events (as in regenerative-braking with HEVs, for example) could be accommodated.

### 3.3. Towards the suppression of hydrogen evolution

Any attempt to suppress the HER by reducing surface-area is likely to be counterproductive because both the capacitive mechanism and the rate of charge have a positive dependency on surface-area. Some control over hydrogen evolution might be exercised by limiting the potential that is applied to the cell via the battery management system. Nevertheless, research efforts to restrict the hydrogen evolution that results from the carbon additions continue to focus on the materials involved (e.g., purity, surface functional groups) and additional solid phases. X-ray photoelectron spectroscopy (XPS) analysis of the chemical composition of carbon samples provided evidence [31] that organic groups can form bonds with organic species close to the surface. As a result, the surface energy and surface properties of carbon can be changed. For instance, bonds to lignosulfonates could explain the dependence between the amount of carbon and the necessary amount of expander, whereas bonds to lead and water could explain not only the differences in the affinity of lead to the carbon surface but also the high affinity of carbon to hydrogen.

In a recent publication [4], it has been reported that the presence of nitrogen-containing groups at the carbon surface increases double-layer capacitance but aggravates the HER. It was therefore suggested, but not tested, that acidic surface groups attached to the carbon surface might diminish the HER. This approach had been included in the research of another group [27], who sought to mitigate the hydrogen reaction in two ways, namely:

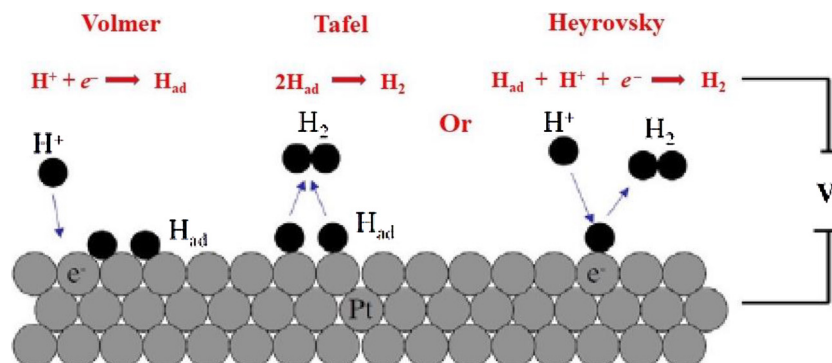


Fig. 8. Alternative mechanisms proposed for hydrogen evolution [27]. For the enquiring reader, a detailed analysis of these mechanisms is given in reference [28].

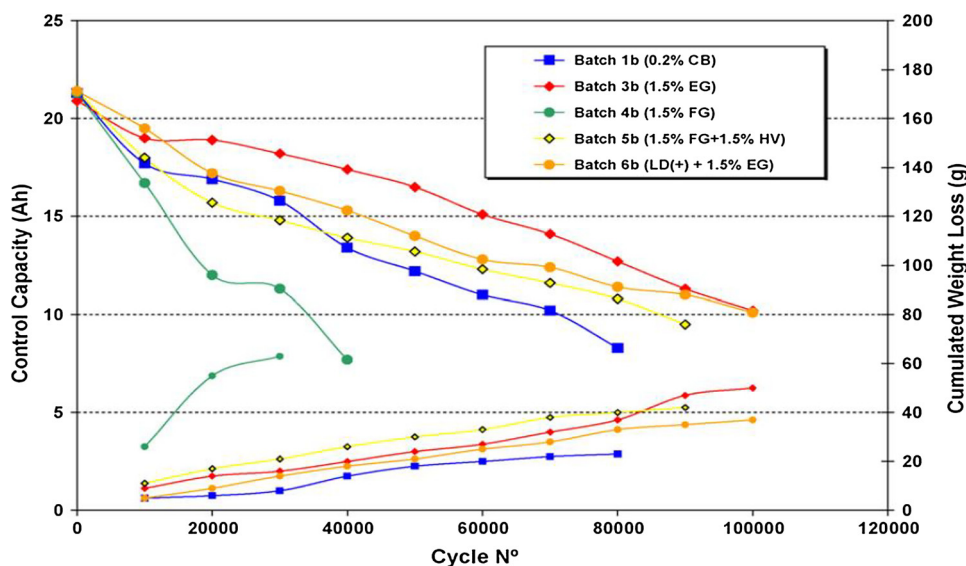


Fig. 9. Weight-loss due to hydrogen evolution from cells that contain different types of carbon. HV is a micro-glass fibre; LD(+) is a low-density expanded graphite [29].

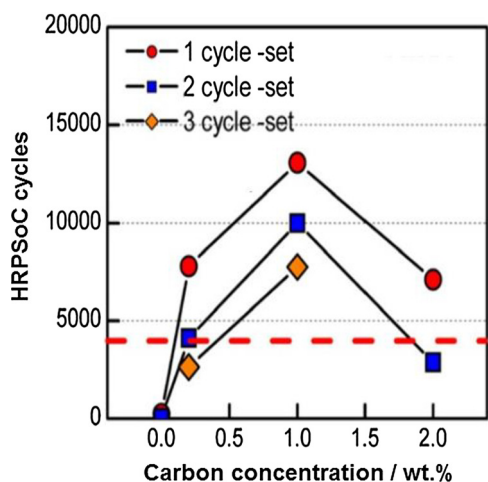


Fig. 10. The beneficial effect of an activated carbon peak ~ 1–2 wt.%. At greater concentrations of carbon, water-loss due to hydrogen evolution takes over [30].

- by reducing the rate of proton adsorption on the carbon surface through making the surface more acidic;
- by affecting the rate of electron transfer from the carbon surface through making the surface either more or less conductive.

These workers showed a strong correlation of normalized HER current with increasing carbon pH but, unfortunately, did not explain the process by which this improvement was achieved.

Surface groups may also play an important part in the changes in negative plate behaviour that result from the addition of graphene oxide (GO) to the active-material. Studies have demonstrated [32] that the rate of hydrogen evolution is increased with 1 wt.% GO, but there is a decrease in the rate when using polypyrrole. Such additives are also said to augment the redox processes between lead and lead sulfate. The authors report a marked increase in the life of a flooded cell when operating under HRPSoC conditions. It should be noted, however, that the test regime was limited to a cycle at 1C or 2C (for 30 s) and it is perhaps significant that the cycle-life at the higher rate was markedly less than that at the lower.

There has also been a suggestion [33] that an increase in the amount of lignosulfonate component of the expander that is conventionally incorporated in the negative active-material can reduce the rate of water loss.

Clearly, on the one hand, the materials should be free of elements that reduce the hydrogen overpotential. On the other hand, it has been found [34] that certain other elements actually serve to suppress the evolution of hydrogen at the negative plate. In a practical example, it has been proposed in a patent document [35] that the carbons used in the UltraBattery™ should be accompanied by lead or zinc.

A detailed exploration of the influence of residual elements on the oxygen- and hydrogen-gassing rates of lead-acid batteries [34] provided a more extended list of metals that presented some promise for limiting hydrogen evolution. For hydrogen gassing, masking effects (‘beneficial synergistic effects’) were found to arise mainly from the combined action of bismuth, cadmium, germanium, silver and zinc. A combination of bismuth, silver and zinc gave the greatest suppression of gassing.

In more recent years, attempts to find metal additives that can resolve the hydrogen evolution (and hence water-loss) problem that arises when extra carbon is added to the negative plate have been pursued with some vigour. For example, when activated carbon (AC) is doped with nano-sized lead particles and added at around 1 wt.% to the negative active-material [36], the HER current is reduced by some 80% in comparison with the level that occurs with activated carbon alone; see Fig. 11. At a potential of -1.36 V, the hydrogen evolution current of

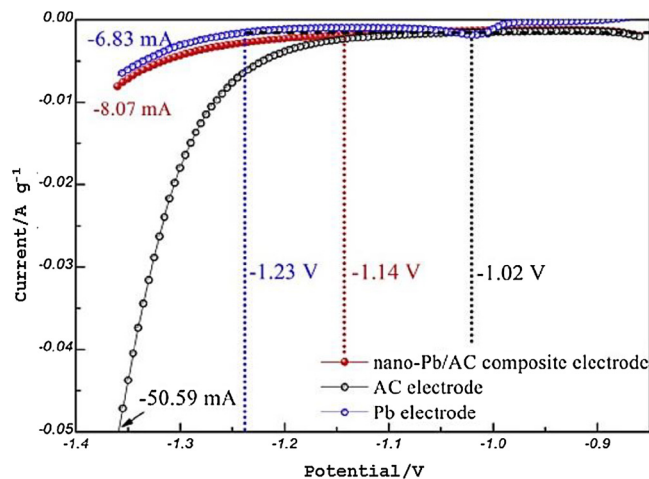


Fig. 11. Linear sweep voltammetry curves for various electrodes (sweep rate: 1.0 mV s<sup>-1</sup>, electrolyte solution: 5M H<sub>2</sub>SO<sub>4</sub>, temperature: 25 °C) [36].

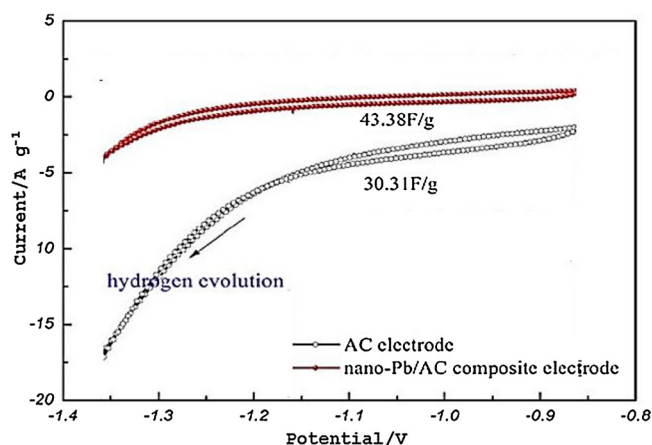


Fig. 12. Current–voltage curves of AC and nano-Pb–AC electrodes (sweep rate:  $10 \text{ mV s}^{-1}$ , electrolyte solution:  $5 \text{ M H}_2\text{SO}_4$ , temperature:  $25 \text{ }^\circ\text{C}$ ) [36].

the nano-Pb–AC electrode is  $-8.07 \text{ mA cm}^{-2}$ , which is only 16% of that for the AC electrode ( $-50.59 \text{ mA cm}^{-2}$ ), but close (118%) to that for the pure lead electrode ( $6.83 \text{ mA cm}^{-2}$ ).

The authors suggest that the presence of the nano-lead assists the mixing of the activated carbon with the lead paste. In the same work, an increase in capacitance of more than 40% was observed, see Fig. 12. Test cells using negative active-material doped with such nano-Pb–AC composites displayed improvements in rapid charge characteristics, high-rate discharge and cycle-life.

Spanish investigators [37] have proposed that it is important for the carbon and lead components of the negative active-material to be in close contact. For example, carbons with a relatively high particle-size that could be introduced into the lead skeleton were able to contribute capacitance to improve DCE and extend life by delaying sulfation. A

### Box 3

#### Pseudocapacitance.

Transition metal oxides undergo electron-transfer reactions but yet behave in a capacitive manner [42]. These materials are said to exhibit ‘pseudocapacitance’ which occurs when ions are electrochemically adsorbed on the surface of a material with a concomitant Faradaic charge-transfer.

Rather than being associated with potential-dependent accumulation of electrostatic charge, as in a double-layer capacitor, the charge is stored indirectly through the Faradaic chemical processes. The speed of the reversible redox reactions is such that the electrochemical features are those of a carbon-based capacitor, but with significantly higher capacitances. The term pseudocapacitance arises because the capacitance is not always constant. Ruthenium oxide is typical example and stores protons from aqueous electrolytes, as presented schematically in Fig. 13. In crystalline form  $\text{RuO}_2$  has a capacity of  $380 \text{ F g}^{-1}$ , in the amorphous or hydrated form it approaches  $800 \text{ F g}^{-1}$ , and in ‘nanodot’ form shows greater than  $1000 \text{ F g}^{-1}$ .

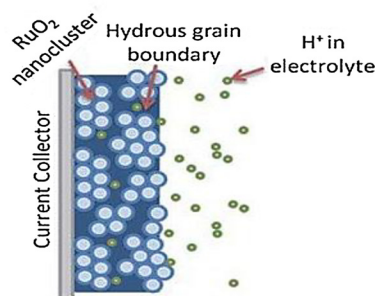


Fig. 13. Illustration of reversible redox reactions that give rise to pseudocapacitance [43].

carbon black, however, remained on the lead surface and cells with this material succumbed to sulfation.

Beneficial effects can also be achieved when Pb(II) ions are intimately combined with activated carbon [21]. The ions, supplied as an aqueous solution of lead nitrate, disperse well in the carbon and the resultant materials exhibit remarkably higher specific capacitance (up to  $250 \text{ F g}^{-1}$ ) and a higher hydrogen overpotential compared with the original carbons. When admixed at a concentration of 1 wt.%, these additives invest the negative active-material with an overall specific capacitance of up to  $2.5 \text{ F g}^{-1}$ , which is a huge step up from that of a counterpart with no supplementary carbon, viz.,  $0.06 \text{ F g}^{-1}$  [38]. The result is again a marked extension in high-rate HRPSoC operation.

There have been several other accounts of the careful admixture of carbon and lead to create beneficial additives for the negative active-material and not all have involved the use of activated carbon. Lead monoxide (PbO) combined with carbon black (CB) has been reported [39] to result in a lower HER than was found with CB alone and, once more, an improvement in HRPSoC cycle-life was obtained. The PbO–CB composites were prepared by pyrolysis and pickling of a CB that had been treated with lead nitrate solution and ammonia. Such treatment endowed the composites with a higher content of alkaline surface functional groups and less carboxyl surface functional groups compared with CB. A 1 wt.% sample of the resultant material was incorporated into the negative active-mass of lead–acid cells to achieve the extended cycle-life.

Another approach has been to form a composite material from lead-doped porous carbon and graphite, which are believed to function synergistically in inhibiting hydrogen evolution and prolonging HRPSoC cycle-life [40]. In a further study, the same authors [41] report that their new nano-lead electrodeposits could contribute superior pseudocapacitance (see Box 3 below) in addition to suppressing the hydrogen evolution induced by carbon.

During operation of a hybrid energy-storage system with a  $\text{PbO}_2$  positive and a carbon negative, Russian workers [44] found that the

carbon collected between 200 and 600 mg Pb per square centimeter of electrode area. It appeared that electroplating of lead occurred fairly rapidly during the early part of service. The uptake of lead by the carbon electrode led to an increase in the specific capacitance of the electrode from 130 to 430 F g<sup>-1</sup>. Based on the observation that the shape of the discharge voltage curve of the electrode does not change appreciably (just its slope), it was assumed that the increase in capacitance was due predominantly to an increase in specific-area capacitance (F cm<sup>-2</sup>) that was associated with the total surface of the deposited lead metal, compared with that of the carbon. Whereas typical (minimum) values for metal surfaces can be as high as 40–60 F cm<sup>-2</sup>, those for different types of carbon are generally lower and can be well below 10 F cm<sup>-2</sup> [45].

Significantly, it has been suggested ([46–48] and see also Section 4.2 below) that basal plane carbon can be treated as a semiconductor and that there is a distribution of charge-carrier concentration that gives rise to a semiconducting space-charge region adjacent to its surfaces. The capacitance of graphite, for example, is then comprised of three components that operate in series, namely: the Helmholtz ( $C_H$ ) and diffuse ( $C_{diff}$ ) double-layers and a space-charge capacitance ( $C_{SC}$ ) within the solid. The space-charge element, which extends into the solid from the interface with the liquid, can be modified by the presence of metal particles (such as the lead particles discussed above) at the surface, as shown schematically in Fig. 14. If the metal is one with a work function that is larger than the electron affinity of the carbon, then the act of bringing the two materials into mutual contact leads to electron flow from the carbon into the metal to bring their Fermi levels into alignment. The remaining positively-charged atoms in the carbon modify the space charge region and this change is expected to alter the hydrogen evolution overpotential. Electron affinity varies considerably from one form of carbon to another [49] so that the beneficial effects on the overpotential of hydrogen evolution are not expected to be universal amongst different types of the material.

To summarize, there is ample evidence that the intimate combination of some forms of carbon with lead metal or lead monoxide can provide additives that invest the negative active-material with enhanced capacitance. This facility results in benefits to the DCE and, at the same time, is able to raise the overpotential of hydrogen evolution and thereby alleviate the problem of water loss.

An investigation [50] has demonstrated that the addition of Zn(II) — either as solid ZnO to a negative active-mass that contains electrochemically active carbon (EAC) or as ZnSO<sub>4</sub> to the electrolyte solution — reduces hydrogen evolution in comparison with a cell containing EAC alone, without any loss of the benefit in charge-acceptance; see Fig. 15.

More recently, the addition of 0.05 wt.% ZnO and 0.5 wt.% carbon black of high surface-area (both by weight of leady oxide) to a conventional negative active-mass has been found to reduce hydrogen

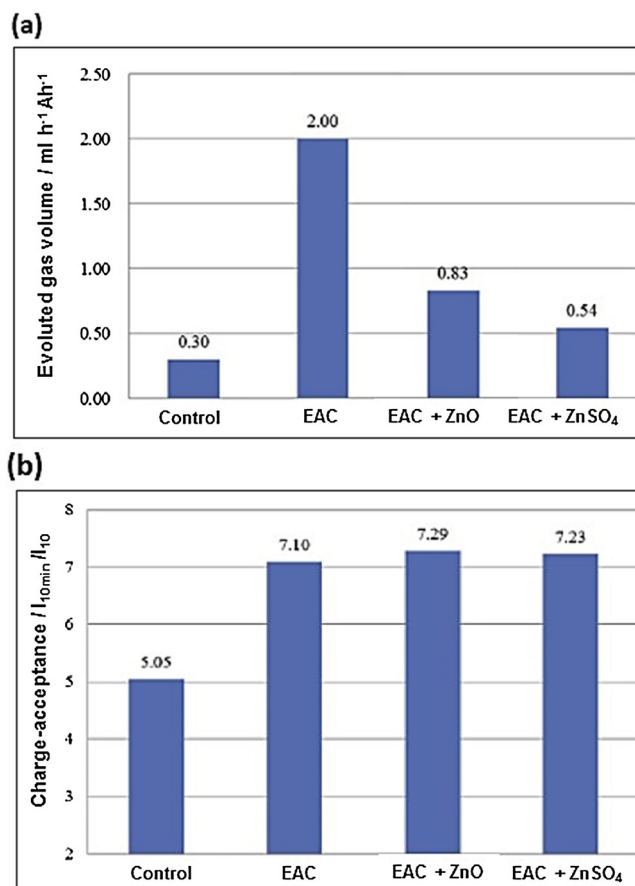
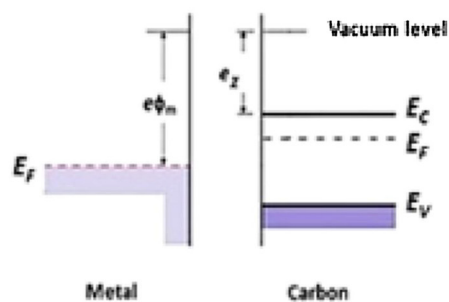


Fig. 15. (a) Hydrogen evolution rates from cells containing EAC, EAC + ZnO and EAC + ZnSO<sub>4</sub> compared with control; (b) charge-acceptance for the same four cells [50].

evolution and improve HRPSoc cycling performance [51]. The ZnO was synthesized by ultrasound-assisted precipitation from a solution of zinc nitrate and potassium hydroxide. Despite these studies, however, zinc has not yet been proved to be as effective as lead (in the appropriate form) in suppressing the HER.

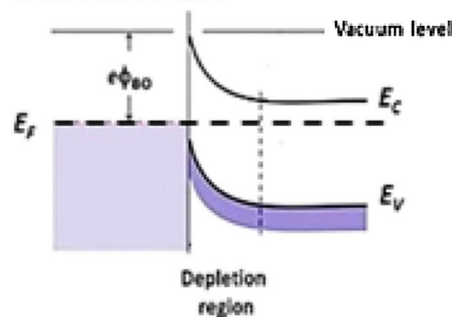
A third metal has now been shown to enhance the value of carbon added to the negative plate. It has been reported [52] that the addition of bismuth sulfide can inhibit hydrogen evolution on lead–carbon negative plates. Negative electrodes modified with a C–Bi<sub>2</sub>S<sub>3</sub> composite exhibited good low-temperature performance. The hydrogen evolution reaction onset potential of a C–Bi<sub>2</sub>S<sub>3</sub> composite electrode was negative-shifted (–1.23 V). Activated carbon modified with 4 wt. % Bi<sub>2</sub>O<sub>3</sub> also

Energy band before contact



(a)

Energy band with metal and carbon in intimate contact



(b)

Fig. 14. Schematic of the contact between a metal (on the left) and a carbon that is behaving as a semiconductor (on the right). (a) Energy band diagram before contact. (b) Energy band diagram with the metal and carbon in intimate contact. The region marked as ‘Depletion region’ carries a positive space charge due to the balancing of the Fermi levels that is achieved by migration of electrons from the carbon into the metal.  $E_f$  Fermi level energy,  $E_v$  energy of the valence band,  $E_c$  energy of the conduction band,  $\chi$  electron affinity,  $\phi_m$  work function,  $\phi_{B0}$  Schottky barrier height.

suppressed hydrogen evolution by negatively-shifting the hydrogen evolution onset potential to  $-1.12$  V. Evidently, C–Bi<sub>2</sub>S<sub>3</sub> is more effective in inhibiting hydrogen evolution than C–Bi<sub>2</sub>O<sub>3</sub> and its excellent behavior is probably due to the more uniform distribution and stronger interaction between C and Bi<sub>2</sub>S<sub>3</sub>.

Notably, both zinc and bismuth appear in the group of elements that were found by CSIRO to reduce negative-plate gassing during float charge [34].

Clearly, the exploitation of metal additives to alleviate the problems of hydrogen evolution deserves further study; see Section 6.

#### 4. Significant properties of carbon

##### 4.1. Structures and electrical conductivity properties of various forms of carbon

Carbon can exist in various forms with a very wide range of physical characteristics that depend very strongly on the respective electronic properties of the atoms. The principal allotropes of the element are:

- (i) diamond, in which the carbon atoms are  $sp^3$ -hybridized so that the material is very hard and electronically resistive;
- (ii) Graphite, in which the atoms are  $sp^2$ -hybridized and invest the material with a softer, layered structure that exhibits significant conductivity along the planes of its hexagonal structure.

Other forms of carbon, e.g., activated carbon and carbon black, generally consist of combinations of  $sp^3$  and  $sp^2$  carbon atoms and exhibit electronic conductivity properties between those of diamond (an insulator) and graphite (a semi-metal) see Fig. 16. The physical properties of the two principal allotropes are listed in Table 1.

In the context of the materials present in the negative plate of a lead–acid cell, it is worth noting that the thermal conductivity of graphite is approximately four times that of lead ( $35.3$  W m<sup>-1</sup> K<sup>-1</sup>) and therefore the presence of graphite will assist heat distribution within the negative active-material. The resistivity of graphite (both parallel to and perpendicular to the basal plane, see Table 1) is greater than that of lead ( $2.08 \times 10^{-7}$  Ω m). Consequently, early theories that the benefits gained by the addition of carbon are due to an improvement in the conductivity of the negative active-material appear to be groundless — except when the electrode is discharged to such an extent that almost all of the sponge lead is replaced by lead sulfate.

The diamond structure tends to exhibit a high degree of crystalline perfection, although isolated point defects can occur. By contrast, the layered structure in graphite allows a range of defect opportunities that give rise to considerable variability in physical properties [53]. The

**Table 1**  
Physical properties of diamond and graphite.

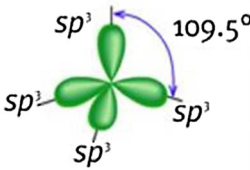
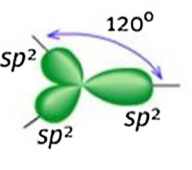
Property	Diamond	Graphite
Crystal structure	Cubic	Hexagonal
Orbital hybridization	$sp^3$	$sp^2$
Covalent radius, pm <sup>*</sup>	77	73
Density, g cm <sup>-3</sup>	3.515	2.267
Mohs hardness	10	~1
Heat capacity, J mol <sup>-1</sup> K <sup>-1</sup>	6.155	8.517
Thermal conductivity, W m <sup>-1</sup> K <sup>-1</sup>	~2200	~150
Resistivity, Ω m	~ $10^{12}$	~ $3 \times 10^{-3}$ (c-axis) ~ $4 \times 10^{-6}$ (a-axis)

\* picometres; 100 pm = 1 angstrom (Å).

normal –AB– layer stacking sequence, in which the atoms of alternate layers in the crystallographic  $c$ -axis sequence are situated identically in the  $x$ - $y$  plane, results in a hexagonal structure. The structure can, however, be re-ordered to construct a rhombohedral sequence –ABC– in which the atoms of every third layer in the  $c$ -axis sequence are situated identically in the  $x$ - $y$  plane. Such re-ordering can be partial or complete. Further, a fraction of the carbon atoms can be  $sp^3$  rather than  $sp^2$  hybridized, with the result that the individual (‘graphene’) layers become buckled. Indeed, the concentration of  $sp^3$  carbons can be quite high [54]. Disordered carbon systems even with the same ratio of  $sp^2$  to  $sp^3$  carbons show a variety of different electronic structures owing to the degree of clustering of  $sp^2$  carbons into ‘graphitic domains’. A disordered distribution of  $sp^2$  sites in a  $sp^2$ - $sp^3$  mixed system disrupts the conjugated electron system even when the concentration of  $sp^3$  carbons is rather low. Such ‘non-graphitic’ disorder serves to reduce conductivity, but this can be restored by thermally-induced migration of  $sp^3$  defects at temperatures from 200 to 400 °C [54]. The degree of crystalline perfection is reduced to a minimum in the production of amorphous or glassy forms of carbon. The ultimate crystallite size for carbon materials can vary over a large range, from 0.001 to 100 μm [55]. Evidently, the specific surface-area of such material can also vary widely.

Departures from the perfect structure of graphite, which can arise from the occurrence of stacking faults and/or the accommodation of  $sp^3$  carbon atoms, cause the conductance of the material to exhibit a wide spread of values [54]. The chemical reactivity of a given carbon material is influenced by the specific area and the composition of the surface. Each  $sp^3$  carbon atom has one free bond that is not involved in holding the graphene layer together. Such bonds can provide attachment to a variety of chemical entities, e.g., carbonyl, carboxyl, lactone, Quinone, phenol and various sulfur and nitrogen species [55].

Two important factors affect the electrochemical behavior of

Diamond	Activated carbon	Graphite
 <p><math>sp^3</math>-hybridization</p>	Carbon blacks	 <p><math>sp^2</math>-hybridization</p>
	Carbon fibres	
	Glassy carbon	
	Carbon aerogels	
	$sp^3/sp^2$ combinations	
Insulator	‘Semiconductor’	Semi-metal

**Fig. 16.** Structures of diamond comprised of  $sp^3$  carbon atoms and of graphite comprised of  $sp^2$  atoms. Other carbons are composed of  $sp^2/sp^3$  mixtures.

graphite, namely, the layered structure and an amphoteric disposition [56]. The layered structure of graphite — which involves strong bonds within the sheets of atoms (the graphene sheets) that lie perpendicular to the *c*-axis and weak bonds between the sheets — allows a rich intercalation chemistry. A wide variety of species can be inserted between the graphene sheets and such intrusions increase the interlayer spacing without disturbing the bonds that hold the sheets together. The earliest graphite intercalation compounds, which entailed the incorporation of potassium, were reported over 160 years ago [57]!

The amphoteric characteristic of graphite arises because graphite is a semi-metal (the valence and conduction bands overlap slightly [58]) in which both electrons and holes are always available to carry current. As a result, graphite can act as an oxidant towards an electron donor intercalate and as a reductant towards electron acceptor species such as acids. Pure graphite intercalation compounds can be synthesized via *n* stages between 1 and at least 12 — as determined by both the nature of the intercalate and the synthesis route. The value of *n* indicates the number of graphene layers between consecutive layers of intercalates. Graphite intercalation compounds can exhibit remarkable properties. For example, the stage-1 lithium graphite intercalation compound has a conductivity of  $2.4 \times 10^5 \text{ S cm}^{-1}$  within the graphene planes and  $1.8 \times 10^4 \text{ S cm}^{-1}$  in the direction perpendicular to the planes [59].

Graphite also forms a number of intercalation compounds with sulfuric acid [60–62]. These develop when the intercalation process is assisted either by the presence of an oxidizing agent (such as  $\text{PbO}_2$ ) or by electrochemical action when the material is held at a positive potential. In general, the process involves the insertion of both  $\text{HSO}_4^-$  ions and neutral  $\text{H}_2\text{SO}_4$  molecules, with the charge on the former balanced by a positive charge on the oxidized graphite network, e.g.,  $\text{C}_{24}^+ \cdot \text{HSO}_4^- \cdot 2.5\text{H}_2\text{SO}_4$ . The stage-1 sulfuric acid graphite intercalation compound (alternating graphene and sulfuric acid layers) can be prepared in 96% acid at a cell voltage just below the decomposition potential of the electrolyte solution [56]. At any particular oxidation level, the graphite bisulfate compound can be decomposed by a cathodic current. In general, the formation of intercalation compounds of graphite results in an increase in electrical conductivity [53].

It has also been reported [63,64] that hydrogen can be stored in carbon single-wall nanotubes by an electrochemical process. Carbon samples subjected to a negative potential in a cell with a potassium hydroxide electrolyte solution and a nickel counter electrode were found to take up 1–2 wt.% of hydrogen that could be released when the potential was reversed. Further, the maximum stored concentration could be increased by incorporating Group I metals (especially, lithium) into the carbon structure [64]. It is not yet clear whether this result signals the feasibility of protonic intercalation into the graphite

structure, but it has been shown [65] that electrodes constructed from carbon fabrics of high surface-area (woven bundles of activated carbon fibre) are able to store reversibly between 1.5 and 2.0 wt.% hydrogen. These authors suggested that the mechanism of storage was indeed intercalation (of nascent hydrogen) into graphitic domains, rather than trapping of hydrogen by carbon-surface functional groups.

In summary, a wide range of amorphous, or poorly crystalline, substances can be prepared in which both *sp*<sup>2</sup> and *sp*<sup>3</sup> carbon atoms are present. Such materials exhibit physical properties, such as electrical conductivity, that are intermediate between those of the diamond and graphite ‘end-members’, but also are strongly influenced by other parameters associated with materials. Their conductivity, for example, depends not only on the ratio of *sp*<sup>2</sup> to *sp*<sup>3</sup> carbon atoms but also on the purity, micro-texture, activation, and thermal pretreatment [66]. The common precursors of carbon capacitor electrodes are coal-tar pitch, coke produced by heating organic materials, and petroleum coke which is the carbonization product of heavy residues in petroleum processing; see Fig. 17. Hard carbons are non-graphitizable and are obtained by carbonizing thermosetting polymers (phenol-formaldehyde resins, furfuryl alcohol, and divinylbenzene–styrene co-polymers), cellulose, charcoal, and fruit shells. Graphitizable carbons are able to form graphite-like structures by heat treatment of petroleum coke, oil, and coal-tar pitch. An intermediate liquid-like ‘mesophase’ facilitates the three-dimensional ordering.

The particle-size of the carbon materials can be anywhere between a few nanometres and tens of microns, whereas surface-areas can vary from a few  $\text{m}^2 \text{ g}^{-1}$  (graphite) to over  $2000 \text{ m}^2 \text{ g}^{-1}$  (activated carbons and carbon blacks). Activated carbon, which is mainly amorphous, consists of flat aromatic sheets, broken in places by slit-formed pores, and of cross-linked amorphous carbon that defines cylindrical pores by its accidental orientation; see Fig. 18. The aromatic character determines the internal resistance of the carbon particles. Ash components (silicon, calcium, magnesium, iron, sodium, potassium, etc.) appear as ions, oxides and other salts, which may be eluted by the electrolyte solution, or may be catalytically active. Heteroatoms (hydrogen, oxygen, nitrogen, sulfur, chlorine, phosphorus) are present in individual particles, as intercalated impurities between the aromatic sheets, or incorporated as functional groups. Such groups dictate the acid character of the material and its ion-exchange properties.

Carbon blacks are composed of agglomerates of interconnected clusters within which there are regions that are ordered and have the graphite structure. In the absence of other factors, electrical conductivity is likely to follow the sequence graphite > carbon blacks > activated carbons. The surfaces of these materials, however, can accommodate a range of atoms or groups of atoms [67] that exercise

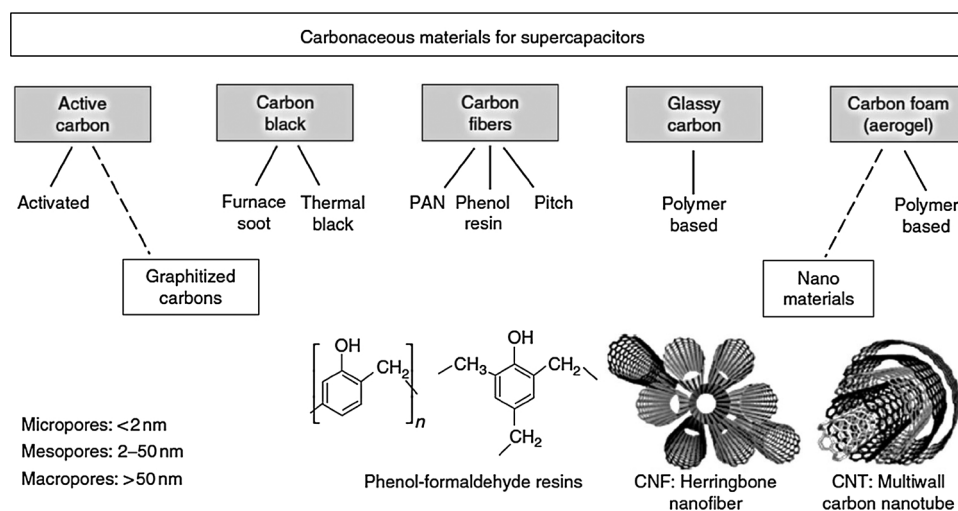


Fig. 17. Carbon materials for supercapacitors [66].

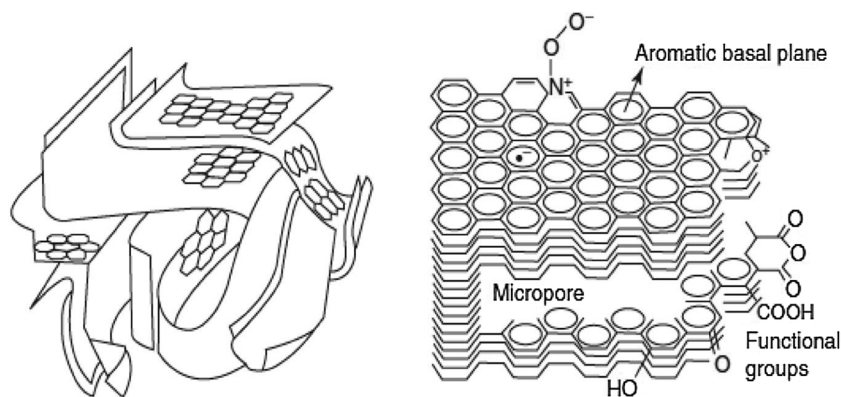


Fig. 18. Structure of activated carbon materials [66].

considerable influence on properties such as wettability, double-layer formation, and chemical reactivity. Impurity levels are equally important. Depending on the production process, industrial carbons can contain up to 10 000 ppm of ‘foreign’ elements that can include various amounts of iron, nickel, copper, zinc, silicon, potassium, and sulfur. In view of the need to restrict the evolution of hydrogen during charging, it is, of course, particularly important to prevent or minimize the presence of those impurities that would promote such gassing.

For VRLA cells, a further criterion in the selection of appropriate carbon additive(s) to the negative active-mass should be their ability during charging to resist attack by the oxygen from the positive that is destined for recombination.

#### 4.2. Capacitive properties of carbon

It has been suggested [30] that the lead electrode in the lead–acid battery may possibly transform into a lead–carbon electrode. For this to occur in practice, the carbon type used as an additive to the negative active-mass should have high affinity for lead. If this is the case, another factor of primary importance is the amount and size of the carbon particles. When the dimensions of the carbon particles are of the order of tens of micrometers, lead nuclei may form on the surface and form a lead–carbon active-material. Activated carbon particles, on the other hand, have high surface-area and a microporous structure. When their pores are filled with water, they acquire the properties of a supercapacitor. Water and  $H^+$  ions penetrate into the carbon pores. During charging, these carbon particles store charge in a capacitive process, which will improve the charge-acceptance of the negative plates.

In a review of the capacitive properties of carbon in supercapacitors [48], it was pointed out that the anticipation that the capacitance of a porous carbon material (expressed in  $F\ g^{-1}$ ) will be proportional to its available surface-area (in  $m^2\ g^{-1}$ ) usually represents an oversimplification [68–70]. The major factors that contribute to what is often a complex (non-linear) relationship are:

- (i) uncertainties in the measurement of electrode surface-area;
- (ii) variations in the specific-area capacitance of carbons with differing morphology;
- (iii) variations in surface chemistry (e.g., wettability and pseudocapacitive contributions);
- (iv) variations in the conditions under which carbon capacitance is measured.

The surface-areas of porous carbons and electrodes are most commonly measured by gas adsorption (usually nitrogen at 77 K) and use BET theory to convert adsorption data into an estimate of apparent surface-area. Despite its widespread use, the application of this approach to highly porous (particularly microporous) and heterogeneous materials has some limitations [71] and is perhaps more appropriately

used as a semi-quantitative tool. Possibly the greatest constraint in attempting to correlate capacitance with BET surface-area, is the assumption that the surface-area accessed by nitrogen gas is similar to that accessed by the electrolyte solution during the measurement of capacitance.

Whereas gas adsorption can be expected to penetrate the majority of open pores down to a size that approaches the molecular size of the adsorbate, electrolyte solution accessibility will be more sensitive to variations in carbon structure and surface properties [72]. Penetration of the solution into fine pores, particularly by larger organic electrolytes, is expected to be more restricted (due to ion-sieving effects) and to vary considerably with the choice of electrolyte [73]. Variations in electrolyte–electrode surface interactions that arise from differing electrolyte properties (viscosity, dielectric constant, dipole moment) will also influence wettability and, hence, penetration into pores.

For carbon-based double-layer capacitors, the presence of surface groups is also known to influence the electrochemical interfacial state of the carbon surface and its double-layer properties that include: wettability, point of zero charge, electrical contact resistance, adsorption of ions (capacitance), and self-discharge characteristics [74,75]. Graphitic carbon surfaces can be regarded as being made up of (at least) two chemically different kinds of sites, namely, basal and edge carbon sites [75]. Edge sites are considered to be more reactive than basal sites as they are often associated with unpaired electrons. This view is supported by the observation that the reactivity of edge sites towards oxygen, for high-purity graphite, is an order of magnitude greater than that of basal sites [76]. Consequently, the chemical properties of carbons also vary with the relative fraction of edge sites and basal plane sites; with the ratio of edge to basal sites generally increasing with the degree of disorder.

The specific-area capacitance (expressed per unit of BET surface-area, in  $\mu F\ cm^{-2}$ ) of a range of carbon materials is listed in Table 2. The values vary considerably and appear to be highly dependent on carbon morphology. Most notably, the capacitance of the edge orientation of graphite is reported to be an order of magnitude higher than that of the

**Table 2**  
Typical values for specific-area capacitance ( $\mu F\ cm^{-2}$ ) of carbonaceous materials [74].

Carbonaceous material	Electrolyte	Capacitance ( $\mu F\ cm^{-2}$ )	Surface area ( $m^2\ g^{-1}$ )
Activated carbon	10% NaCl	19	1200
Carbon black	1M $H_2SO_4$	8	80 - 230
	31 wt% KOH	10	
Graphite cloth	0.168 N NaCl	10.7	630
Graphite basal plane edge plane	0.9 N NaF	3	50 - 70
		50 - 70	
Glassy carbon	0.9 N NaF	13	
Carbon aerogel	4 M KOH	23	650

basal layer [77,78]. One determinant of specific-area capacitance could therefore be the relative density of edge and basal plane graphitic structures in carbon materials. Carbons with a higher percentage of edge orientations would be expected to exhibit a higher capacitance.

The low capacitance recorded when the basal layer of graphite is exposed to solution has been examined in detail [46,47]. By treating basal plane carbon as a semiconductor, there resulted a distribution of charge-carrier concentration (charge density) that gave rise to a semi-conducting region of space charge on the carbon side of the interface. This means that some of the applied potential extends into the carbon and a space-charge capacitance ( $C_{sc}$ ) develops. This capacitance is in series with other capacitive components of the double-layer, namely, the Helmholtz ( $C_H$ ) and diffuse ( $C_{diff}$ ) double-layer contributions. In effect, the stored charge at a given potential is spread over an additional dielectric element. The overall capacitance of the electrode ( $C$ ) is then represented as:

$$\frac{1}{C} = \frac{1}{C_{sc}} + \frac{1}{C_H} + \frac{1}{C_{diff}} \quad (2)$$

For the semiconducting basal graphite layer, the space-charge capacitance is significantly less than  $C_{diff}$  and  $C_H$ , and therefore dominates the overall interface capacitance. In fact, calculations have shown [46,47] that at the point of zero charge essentially all of the potential is associated with the space-charge region within the carbon electrode. By contrast, the edge orientation of graphite has a higher charge-carrier density since its conductivity is more like that of a metal. The space-charge capacitance is correspondingly greater so that the overall interface capacitance is now dominated by  $C_{diff}$  and  $C_H$ .

The measurement of carbon capacitance is also very dependent on the experimental conditions employed. For example, the capacitance values measured for a range of porous carbons can vary substantially with discharge current [79]. The capacitance of microporous carbons is particularly affected by variations in discharge current due to the greater possibility of restricted electrolyte diffusion in narrower pores. Ideally, reported capacitance values of carbon electrodes, particularly when used for comparative purposes, should be measured and evaluated at a fixed current density.

### 5. A model for the lead–carbon negative electrode

In an electrochemical system, a charge zone is formed at the boundary between the electrode and the electrolyte solution. This charged zone provides a double-layer capacitance. As the capacitance is on the surface of the electrode, it occurs in parallel with the electrochemical charge-transfer (Faradaic) reaction, as shown schematically in Fig. 19. The current through the battery  $I_{bat}$  is divided into a part that flows in the charge-transfer reaction and a part that flows into the double-layer capacitor. As the capacitor has a limited storage capability, it is mainly charged just at the first moment of a charge pulse.

In the equivalent circuit displayed in Fig. 19, the voltages of the two elements are equal at all times [80]. Hence:

$$V_{Bat,0} - I_{CT}R_{CT} = V_{Bat,0} - I_C R_C - \int I_C/C \, dt \quad (3)$$

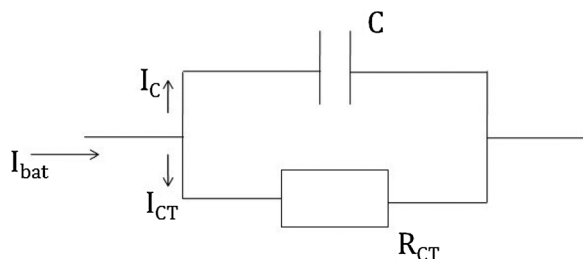


Fig. 19. Equivalent circuit of an active mass with a significant capacitive element.

where subscripts CT refer to the charge-transfer component (Pb–PbSO<sub>4</sub>) and subscripts C refer to the carbon component. Subscript 0 refers to time zero.

Differentiating Eq. (3) gives:

$$-(dI_{CT}/dt)R_{CT} = -(dI_C/dt)R_C - I_C/C \quad (4)$$

Since  $I_{Bat} = I_{CT} + I_C$  and the battery current,  $I_{Bat}$ , is assumed to be constant:  $(dI_{CT}/dt) = -(dI_C/dt)$  and Eq. (4) then becomes:

$$(dI_C/dt) [R_{CT} + R_C] = -I_C/C \quad (5)$$

Integrating Eq. (5) gives:

$$I_C/I_{C,0} = \exp(-t/RC') \quad (6)$$

where  $RC' = C(R_{CT} + R_C)$ . Now, at  $t = 0$ ,  $I_{CT,0}R_{CT} = I_{C,0}R_C$  so that:

$$I_{C,0} = I_{Bat} [R_{CT}/(R_{CT} + R_C)] \quad (7)$$

Eq. (6) can be integrated to obtain an expression for the capacitive charge,  $Q$ , transferred to the carbon, namely:

$$Q = I_{C,0} (RC') [1 - \exp(-t/RC')] \quad (8)$$

where  $RC'$  is the effective time constant of the capacitive element.

By way of example, 35 g of negative active-material containing 2 wt.% of a carbon with a specific capacitance of 150 F g<sup>-1</sup> and specific resistance of 0.001 Ω g<sup>-1</sup> would yield an electrode with 0.7 g of carbon, a capacitance of 105 F and a resistance of 0.15 Ω. Assuming the resistance of the plate is 0.015 Ω, then the time constant of the electrode would be 1.5 s. From Eq. (7), the initial current  $I_{C,0}$  into the capacitive element is found to be 95.5% of the total current  $I_{Bat}$  and charging of the capacitor will be complete in around five times the time constant (v.s.), i.e., 7.5 s (see Box 1, above). This rapid response is the key to the ‘buffering’ effect through which the carbon protects the electrode against high-rate charge pulses and enables the Faradaic component of the behaviour of series-connected cells to remain balanced.

A schematic diagram for the buffering effect of the capacitance [20] is shown in Fig. 20. The large BET surface-area of the activated carbon is considered to form an extensive electric double-layer, which is able to store protons and electrons very rapidly during high-rate charge–discharge conditions. Therefore, during HRPSoc cycling, the Faradaic phase transition of Pb to PbSO<sub>4</sub> and the non-Faradaic charge adsorption–desorption processes take place simultaneously in the negative electrode. Supposing the phase transition between Pb and PbSO<sub>4</sub> is represented by an electric component, R, and the charge adsorption and desorption by an electric component C, then the negative electrode that contains activated carbon can be treated as thousands of parallel R–C micro-circuits.

At the onset of a high-rate charge, the activated carbon acts as an effective buffer of peak power and accepts much of the transient current that would otherwise give rise to hydrogen evolution; see Fig. 20(a). As charging proceeds, the capacitor becomes fully-charged and the external circuit then delivers electrons for the reduction of lead sulfate to lead metal. At this time, the current flowing through the non-Faradaic part decreases to zero; see Fig. 20(b). When the external charge is discontinued, see Fig. 20(c), the electrons stored in the capacitance at the active surface of carbon are discharged to continue the Faradaic charge reaction.

In summary, the capacitive element absorbs high-rate charging for a short time and the Faradaic part of the cell accommodates events that take place over a longer time-scale.

### 6. Maximizing the benefits of carbon

A critical analysis has been undertaken of the possible avenues whereby the addition of supplementary carbon to the negative plate of a lead–acid battery moderates, without exacerbating hydrogen

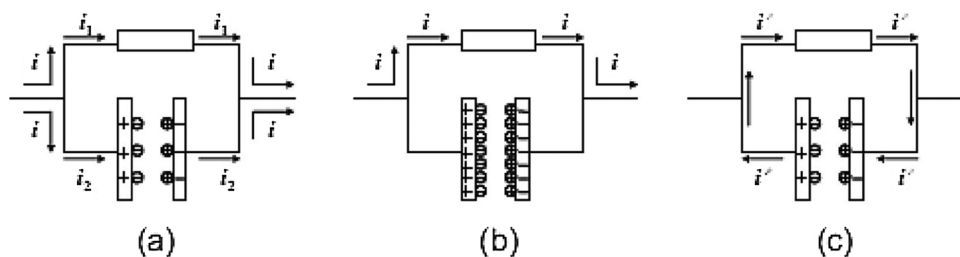


Fig. 20. Buffering mechanism provided by a capacitive element: (a) initial stage of charge; (b) steady stage of charge; (c) the stage after charge [20].

evolution, the development of irreversible sulfation during HRPSoC cycling. It is concluded that:

- (i) a key attribute of carbon is to increase the overall specific capacitance of the negative active-material;
- (ii) given the present state-of-the-art, the beneficial action peaks at additions between 0.5 and 2.0 wt.%.

The addition of extra carbon to the negative active-mass of lead–acid automotive batteries extends the operational life in HRPSoC duty and, in the case of batteries of higher voltage used in hybrid electric vehicles, serves to keep the individual, series-connected, cells well-balanced.

A secondary, but undesirable, consequence of such additions is a reduction in the hydrogen evolution overpotential that leads to loss of

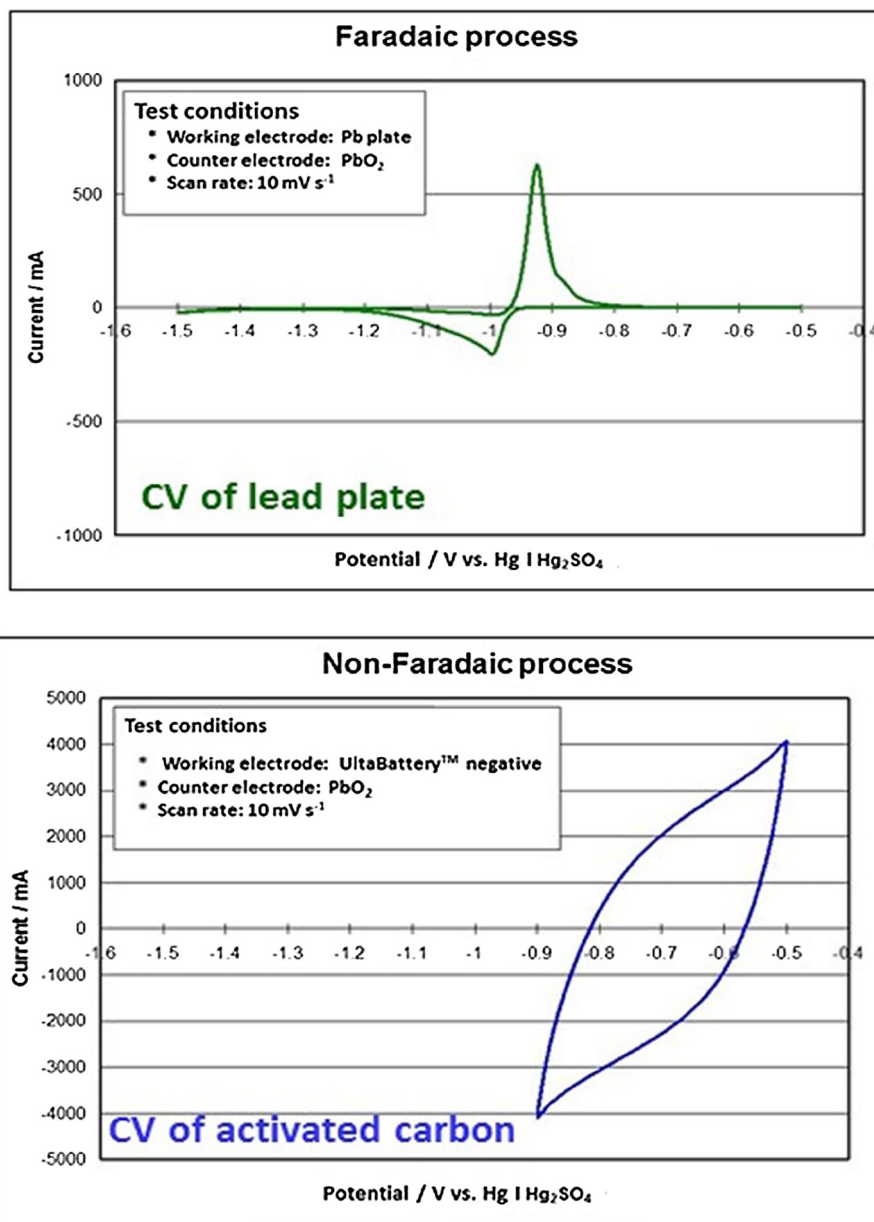


Fig. 21. Cyclic voltammetric (CV) scans demonstrating the operation of the negative plate in an UltraBattery™ [24].

water from the electrolyte solution and a limitation to the beneficial effects that the carbon is intended to provide. Thus, during HRPSoC duty, extra carbon appears to improve dynamic charge-acceptance but may not improve dynamic charge-efficiency as a result of the parasitic reaction evolving hydrogen, with subsequent dry-out causing the early failure of valve-regulated lead–acid batteries.

Without judicious practice, both the benefits of adding carbon and the stumbling block of hydrogen evolution are expected to carry over into lead–acid batteries in stationary energy storage. One or more of the following mechanisms may serve to provide the improvement that, in some cases, carbon brings.

### 6.1. Capacitance

The extra carbon, either admixed with the sponge lead (e.g., Pavlov [81]) or in the form of a porous sheet as in the UltraBattery™ (e.g., Furukawa [24]) introduces the characteristic properties of a capacitor in parallel with the Faradaic reaction; see Fig. 21.

The positive plate in a lead–acid battery is inherently blessed with an anomalously high specific capacitance ( $\sim 7 \text{ F g}^{-1}$ ), which enables it to provide the ‘buffer mechanism’ during HRPSoC charge and discharge without assistance.

By contrast, the raw active-material on the negative plate (sponge lead) has a low surface-area and a specific capacitance of only  $0.06\text{--}0.08 \text{ F g}^{-1}$  and sulfates during HRPSoC duty. When, however,  $\sim 2 \text{ wt.}\%$  of a carbon that is characterized by  $\sim 200 \text{ F g}^{-1}$  is added, the mixture has a specific capacitance ( $4 \text{ F g}^{-1}$ ) that is now comparable with that of the positive. This elevation of the overall specific capacitance of the negative active-material is sufficient to provide the acceptance of  $4 \text{ A s g}^{-1} \text{ V}^{-1}$  which represents 1–2% of the total capacity of the active-material on the plate. During regenerative-braking, only about 2% of the capacity of the battery is used (at the very high rate of charge) and so 1–2 wt.% of carbon provides sufficient capacitance to absorb the greater part of this super high-rate charge. In other words, during the HRPSoC duty for the battery in a HEV, a substantial fraction of the high-rate cycling can be handled by the charging and discharging of the capacitance. Further, the time constant for the capacitive contribution (of the order of seconds) ensures that, the involvement of the capacitive element is complete before there is much contribution from the Faradaic reaction. Consequently, the problem of sulfation can be avoided.

### 6.2. Extended electrochemically-active surface-area

Adding carbon can increase the specific surface-area of the active-material by up to an order of magnitude. Provided that the carbon involved has sufficient electronic conductivity, the increase in surface-area can result in a significant increase in the rates of the electrochemical reactions during charge and discharge.

### 6.3. Physical effects

In cases where the ultimate failure mode of the negative plate is an accumulation of ‘hard’ lead sulfate, the addition of some forms of

carbon may obstruct the growth of lead sulfate crystals that occurs via ‘Ostwald Ripening’ and ensure that the recharge of lead sulfate back to lead is able to continue.

Other possibilities are that carbon admixed with the negative active-material can assist the diffusion of the electrolyte solution through the pore structure of the plate, and that separate sheets of porous carbon in contact with the external surface of the plate can limit the extent of acid stratification. The influence of the way in which the supplementary carbon is incorporated is summarised in Table 3 below.

If the hydrogen evolution problem could be ameliorated then the constructive influence of carbon addition in existing applications (HRPSoC) would be improved and the way could be opened to other duty cycles in which larger amounts of carbon could contribute higher levels of capacitance.

As noted, most of the work devoted to the use of extra carbon in the negative active-mass has been aimed at improving the DCE and extending the life of 12-V batteries for micro-HEVs. In stationary applications of energy storage, however, battery voltages generally need to be much greater than 12 V. If the buffering mechanism that appears to be largely responsible for the improved DCE and life extension of automotive batteries is also accountable for the self-balancing of high-voltage modules during mild-/medium-hybrid vehicle duty, then there should be considerable value in also maximizing the extra-carbon effect for batteries in stationary energy-storage applications.

Optimization of carbon additions should continue and this should include close attention to the effects of active groups at the particle surfaces. Furthermore, there deserves to be a thorough investigation of the potential additional benefits that can be provided by the inclusion of one or more of the metallic elements that appear to enable the suppression of hydrogen evolution.

A ‘volcano plot’ of the hydrogen evolution reaction in acid solution as catalyzed by different metals is shown in Fig. 22 [82]. It is seen that sp metals are located on the left-hand branch of the volcano. They adsorb hydrogen rather weakly and hydrogen is evolved via a rate-determining primary discharge. This branch includes also the metals of the IB group (copper, silver, and gold).

All transition metals are located on the right-hand branch of the volcano. For these metals, the adsorption of hydrogen is strong and the surface concentration is close to saturation, thus making hydrogen evolution difficult.

Precious metals are found in the intermediate range of M–H bond strength. For these, the M–H bond strength is close to the H–H bond strength, i.e., neither too weak nor too strong, according to the qualitative principle of Sabatier in catalysis, and the reaction may proceed at high rate with a mechanism that produces a low Tafel slope. Platinum is in fact among the best catalysts for electrolytic hydrogen evolution.

The position of nickel, iron, and cobalt is a debated issue. If  $\Delta G(\text{M–H})$ , the increase in M–H bond strength, taken from gas-phase experiments is used, these metals are located on the descending branch. In the other hand, when  $\Delta G(\text{M–H})$  is estimated from in situ electrochemical experiments, they appear on the ascending branch. This apparent contradiction can be reconciled if it is considered that  $\Delta G(\text{M–H})$  becomes weaker if hydrogen is absorbed, as occurs during electrolytic hydrogen evolution.

**Table 3**

Configurations of the lead–acid battery in which the several beneficial carbon mechanisms might contribute.

Mechanism	Carbon mixed with lead in a VRLA cell	Carbon mixed with lead in a flooded cell	Separate carbon sheet connected in parallel
Capacitance	Yes	Yes	Yes
Expanded electrochemical reaction surface-area	Yes	Yes	Probably not
Blocking of sulfate crystal growth	Yes	Yes	No
Inhibition of stratification	No	No	Yes

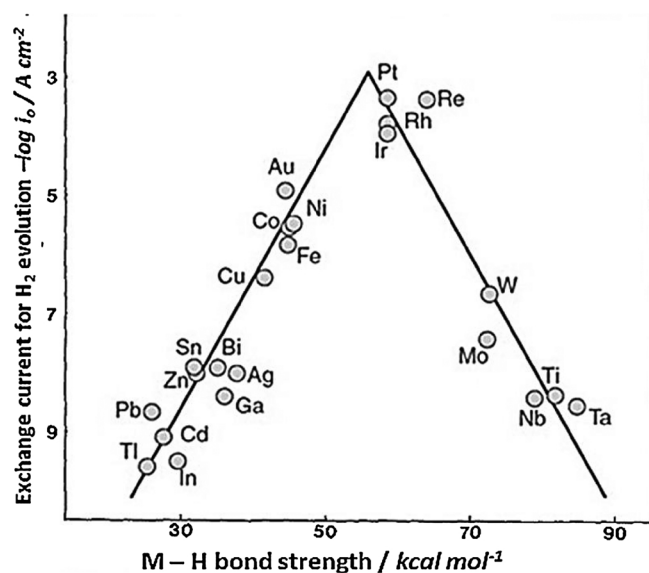


Fig. 22. Exchange-currents for hydrogen evolution vs. strength of intermediate metal–hydrogen bond for different metals in acid solution [82].

The five metals bismuth, cadmium, germanium, silver and zinc (identified by CSIRO [34] and also discussed in Section 3.1) that show promise in limiting gassing from the negative plate of a lead–acid cell are grouped together. As reviewed herein, the merits of lead, zinc and bismuth in suppressing the hydrogen evolution reaction on carbon additives to the negative plate have already been demonstrated. The observation that lead and bismuth also augment the specific capacitance of the carbon is a bonus. Evidently, there is considerable scope for further work in pursuit of increased efficacy of carbon additions.

The overpotential (for hydrogen evolution) acts like a heterogeneous catalyst in that it dictates the rate at which the (hydrogen evolution) reaction proceeds. The presence of particles of certain metals on the carbon surface controls the overpotential in the same way that the presence of certain other metals controls the catalysis of gas-phase reactions on the surface of semiconducting oxides (e.g.,  $\text{SnO}_2$ ,  $\text{CeO}_2$ ). The difference is that, in the case of carbon-enhanced lead–acid batteries, the search is for metal particles that exercise a negative influence on the reaction rate, whereas normally in heterogeneous catalysis metal particles are intended to accelerate reaction rate. Perhaps that is why it is the base metals, zinc, bismuth, lead, that are found to be useful.

## 7. Key findings

The duty cycle to which a battery is exposed is an important factor in controlling the function of supplementary carbon added to the negative active-mass. When the quantity of carbon is of the order of a few wt.% of the active-material, the capacitance mechanism can cope with charging and discharging up to a few percent of the capacity of a lead–acid cell in around 5 s. Such a cycling regime is typical of the schedule to which the battery is exposed during most regenerative-braking events. There is then inadequate time for the Faradaic capacity of the cell, even operating through the extended surface-area, to make a significant contribution. The acceptance of charge by the capacitance at very high rates avoids the danger of any excess charge current spilling over into the parasitic reaction of hydrogen evolution and thereby may leave lead sulfate unreduced.

Duty cycles where the charge and discharge events last much longer than 5 s, however, may still involve charging or discharging the capacitance initially but depend on the Faradaic reaction to access a greater fraction of the overall cell capacity. In such cases, the extended surface-area provided by the carbon material allows charge to be accepted by the Faradaic reaction at higher rates than when the carbon is not

Table 4

Overpotentials (referred to a standard hydrogen electrode) of metals for the hydrogen evolution reaction (HER).

Platinized platinum	Silver	Graphite	Lead	Zinc
–0.07 V	–0.22 V	–0.62 V	–0.71 V	–0.77 V

present. Thus, once again, the threat of hydrogen evolution and reduced DCE is diminished.

In either brief or more extended duty cycles, the presence of carbon can help to prevent the development of so-called ‘hard sulfate’ by obstructing the process of Ostwald ripening.

Unfortunately, given that the hydrogen evolution overpotential on carbon is below that on lead (see Table 4 below), the presence of the extra carbon gives rise to an increase in the loss of hydrogen which, in turn, causes ‘dry-out’ of the electrolyte solution that ultimately leads to cell failure.

The hunt for methods of limiting hydrogen evolution currently represents an active area of research. Detailed evaluation of published work suggests that the following two approaches are the most promising.

### 7.1. Introducing metal-based additives

The addition of certain metals can alleviate the hydrogen loss without degrading the benefits that carbon brings. For instance, it has been found that the incorporation of lead (either as nano-sized lead particles or as lead monoxide), zinc (either as zinc oxide or zinc sulfate) or bismuth (either as sulfide or oxide) in the supplementary carbon serves to restore the hydrogen overpotential and thereby diminishes the HER, as shown for example in Fig. 11 (v.s.).

The role of the added metals can be explained as follows. The hydrogen evolution reaction



is the cathodic reaction in the electrochemical splitting of water and is one of the principal means of producing hydrogen for use as a reagent or as a fuel. In such technology, a catalyst is used to lower the HER overpotential and thus achieve high energy efficiency. Platinum is one of the most effective electrocatalysts for the process (see Table 4 above) as it requires a very small overpotential, even at very high rates in acidic solutions.

Pursuit of the efficient charging of a lead–acid cell, however, demands exactly the opposite outcome and must depend on a surface that offers the highest possible overpotential in order to minimize hydrogen gassing — in fact a ‘negative catalytic effect’. The manner in which the addition of certain metals restores the overpotential that is lost when supplementary carbon is included in the negative active-mass involves an electronic interaction with the carbon surface. This requirement is akin to the metal–support interaction that occurs in gas-phase heterogeneous catalysis. The electronic properties vary a good deal from diamond (insulator), through carbon black, carbon fibres and other allotropes to the very anisotropic graphite (a semi-metal), as illustrated in Fig. 16 (v.s.).

Forms of carbon that are composed of mixtures of  $sp^2/sp^3$  hybridized carbon atoms can behave as semiconductors and undergo Fermi-level equalization with metal particles that are in intimate contact with the carbon surface. Acting in this way, metals with a high HER overpotential can markedly suppress the rate of hydrogen evolution at the carbon surface.

### 7.2. Action of functional groups

Certain functional groups at the carbon surface appear to be capable of reducing the hydrogen reaction by discouraging the rate of proton adsorption. Consistent with this hypothesis is the observation of a

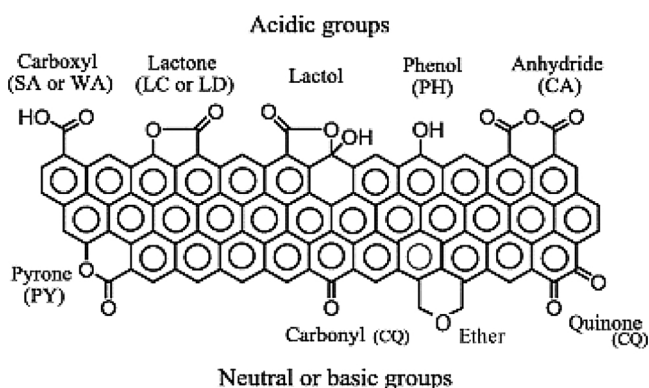


Fig. 23. Active functional groups that can be accommodated at the periphery of a graphene sheet [83].

strong positive correlation of normalized HER current with the increasing ability of functional groups (examples shown in Fig. 23) to render the surface of the carbon more alkaline.

Surface groups may also play an important part in the changes in behaviour of the negative plate that result from the addition of graphene oxide (GO) to the active-mass. As reported recently [84], GO materials that contain a large number of carbon-oxygen single-bond groups promote hydrogen evolution and the reduction of lead sulfate, whereas GO with a high proportion of C=O double-bond groups actually extend the operational life of lead-acid cells in HRPSoc operation.

## 8. Future avenues of research

Although the addition of small amounts of certain carbons to the raw negative active-material takes care of sulfation, hydrogen evolution is aggravated. The benefits of adding up to around 2 wt.% (varying somewhat with the type of carbon) of such carbons to the raw negative active-material outweigh the deleterious effects of hydrogen evolution. At carbon levels above 2 wt.%, however, there is no further benefit because the sulfation has already been suppressed but hydrogen evolution continues to increase pro rata and so battery life decreases.

The rate of the HER (Eq. (1)) depends upon the supply of the reactants, electrons and protons, to the reaction site. The supply of these reactants can be controlled, respectively, by the choice of metal additions and surface functional groups.

Metals that can modify the electrocatalytic evolution of hydrogen on carbon do so by affecting the rate of electron transfer from the carbon surface. To date, only lead, zinc and bismuth have been found to reduce hydrogen evolution on carbon. The CSIRO study of 17 'residual elements' identified bismuth, cadmium, germanium and zinc as being 'beneficial' in reducing hydrogen gassing during float charge [34]. Trasatti's 'volcano curve' indicates that indium, cadmium, lead, gallium, zinc, tin and bismuth all have similar hydrogen evolution properties [82]. Undoubtedly, there is room for further investigation here.

Future work should complete the survey of metals that can effectively increase the HRE overpotential and the optimum manner in which such additives should be deployed. Simultaneously, mitigation of hydrogen evolution by incorporation of functional surface groups on different types of carbon should be evaluated systematically. Obviously, in undertaking modifications of the negative active-mass, it is imperative to safeguard against any adverse influence on the performance of the corresponding positive plate.

## Acknowledgements

This study was made possible through support from ABERTAX Technologies Ltd., Paola, Malta. The authors are also grateful to P.

Atanassova, N. Barsan, A. Burke, H. Giess, A.E. Hughes and E. Meissner for helpful discussions and information.

## References

- [1] K. Peters, Negative plates in valve-regulated lead-acid batteries, in: D.A.J. Rand, P.T. Moseley, J. Garche, C.D. Parker (Eds.), *Valve-Regulated Lead-Acid Batteries*, Elsevier, Amsterdam, The Netherlands, 2004, pp. 135–162 ISBN:0-444-50746-9.
- [2] K. Nakamura, M. Shiomi, K. Takahashi, M. Tsubota, Failure modes of valve-regulated lead-acid batteries, *J. Power Sources* 59 (1996) 153–157.
- [3] M. Shiomi, T. Funato, K. Nakamura, K. Takahashi, M. Tsubota, Effects of carbon in negative plates on cycle-life performance of valve-regulated lead-acid batteries, *J. Power Sources* 64 (1997) 147–152.
- [4] B. Bozkaya, J. Settelein, G. Sextl, Approach to lower water consumption: modified carbon materials for lead-acid batteries, 18th Advanced Automotive Battery Conference (2018).
- [5] K. Kogure, M. Tozuka, T. Shibahara, S. Minoura, M. Saka, Development of lead-acid batteries for idling stop-start system (ISS) use, 9th International Conference on Lead-Acid Batteries, LABAT'2014 (2014).
- [6] P.T. Moseley, D.A.J. Rand, K. Peters, Enhancing the performance of lead-acid batteries with carbon — in pursuit of an understanding, *J. Power Sources* 295 (2015) 268–274.
- [7] J. Settelein, J. Oehm, B. Bozkaya, H. Leicht, M. Wiener, G. Reichenauer, G. Sextl, The external surface-area of carbon additives as key to enhance the dynamic charge-acceptance of lead-carbon electrodes, *J. Energy Storage* 15 (2018) 196–204.
- [8] P.T. Moseley, Consequences of including carbon in the negative plates of valve-regulated lead-acid batteries exposed to high-rate partial-state-of-charge operation, *J. Power Sources* 191 (2009) 134–138.
- [9] E. Karden, S. Buller, R.W. De Doncker, Frequency domain approach to dynamical modeling of electrochemical power sources, *Electrochim. Acta* 47 (2002) 2347–2356.
- [10] J. Settelein, The external surface-area of carbon additives — a key to enhance the dynamic charge acceptance of lead-carbon electrodes, 18th Advanced Automotive Battery Conference (2018).
- [11] V. Srinivasan, G.Q. Wang, C.Y. Wang, Mathematical modelling of current-interrupt and pulse operation of VRLA cells, *J. Electrochem. Soc.* 150 (2003) A316–A325.
- [12] J. Newman, Ohmic potential measured by interrupter techniques, *J. Electrochem. Soc.* 117 (1970) 507–508.
- [13] A. Jaiswal, S.C. Chalasani, The role of carbon in the negative plate of the lead-acid battery, *J. Energy Storage* 1 (2015) 15–21.
- [14] D. Samuelis, A unique functional carbon additive for electrochemical energy storage devices, 16th Asian Battery Conference (2015).
- [15] D. Pavlov, T. Rogachev, P. Nikolov, G. Petkova, Mechanism of action of electrochemically active carbons on the processes that take place at the negative plates of lead-acid batteries, *J. Power Sources* 191 (2009) 58–75.
- [16] D. Pavlov, P. Nikolov, Capacitive carbon and electrochemical lead electrode systems at the negative plates of lead-acid batteries and elementary processes on cycling, *J. Power Sources* 242 (2013) 380–399.
- [17] P. Bača, K. Micka, P. Křivík, K. Tonar, P. Tošer, Study of the influence of carbon on negative lead-acid battery electrodes, *J. Power Sources* 196 (2011) 3988–3992.
- [18] K. Micka, M. Calábek, P. Baja, P. Křivík, R. Labus, R. Bilko, Studies of doped negative valve-regulated lead-acid battery electrodes, *J. Power Sources* 191 (2009) 154–158.
- [19] P. Křivík, K. Micka, P. Bača, K. Tonar, P. Tošer, Effect of additives on the performance of negative lead-acid battery electrodes during formation and partial-state-of-charge operation, *J. Power Sources* 209 (2012) 15–19.
- [20] J. Xiang, P. Ding, H. Zhang, X. Wu, J. Chen, Y. Yan, Beneficial effects of activated carbon additives on the performance of negative lead-acid battery electrode for high-rate partial-state-of-charge operation, *J. Power Sources* 241 (2013) 150–158.
- [21] P. Tong, R. Zhao, R. Zhang, F. Yi, G. Shi, A. Li, H. Chen, Characterization of lead(II)-containing activated carbon and its excellent performance of extending lead-acid battery cycle-life for high-rate partial-state-of-charge operation, *J. Power Sources* 286 (2015) 91–102.
- [22] S.V. Baker, P.T. Moseley, A.D. Turner, The role of additives in the positive active mass of the lead-acid cell, *J. Power Sources* 27 (1989) 127–143.
- [23] A.F. Hollenkamp, Carbon additives, in: J. Garche, C. Dyer, P.T. Moseley, Z. Ogumi, D.A.J. Rand, B. Scrosati (Eds.), *Encyclopedia of Electrochemical Power Sources*, Vol. 4 Elsevier, Amsterdam, The Netherlands, 2009, pp. 638–647 ISBN: 978-0-444-52093-7.
- [24] J. Furukawa, K. Smith, L.T. Lam, D.A.J. Rand, Towards sustainable road transport with the UltraBattery™, in: J. Garche, E. Karden, P.T. Moseley, D.A.J. Rand (Eds.), *Lead-Acid Batteries for Future Automobiles*, Elsevier, Amsterdam, The Netherlands, 2017, pp. 349–391 ISBN: 978-0-444-63700-0.
- [25] P. Atanassova, M. Oljaca, P. Nikolov, M. Matrakova, D. Pavlov, Performance additives for advanced lead-acid battery applications, 15th Asian Battery Conference (2013).
- [26] L.A. Riley, A.J. Sakshaug, A.M. Feaver, Characterization of Carbons and Understanding Their Hydrogen Gassing Properties in Lead-acid Battery Negative Plates, ALABC Research Project 1012L Final Report, ALABC, Durham, NC, USA, (2012).
- [27] A. DuPasquier, A. Korchev, D. Miller, B. Merritt, P. Atanassova, M. Oljaca, Carbon Black Surface Modifications for Reduced Hydrogen Evolution, LABAT' 2017, Golden Sands Resort, Bulgaria, 13–16 June (2017).
- [28] A.R. Kucernak, C. Zalis, General models for the electrochemical hydrogen

- oxidation and hydrogen evolution reactions: theoretical derivation and experimental results under near mass-transport free conditions, *J. Phys. Chem. C* 120 (2016) 10721–10745.
- [29] M. Fernández, J. Valenciano, F. Trinidad, N. Muñoz, The use of activated carbon and graphite for the development of lead–acid batteries for hybrid vehicle applications, *J. Power Sources* 195 (2010) 4458–4469.
- [30] D. Pavlov, P. Nikolov, T. Rogachev, Influence of carbons on the structure of the negative active-material of lead–acid batteries and on battery performance, *J. Power Sources* 196 (2011) 5155–5167.
- [31] B. Monahov, The beneficial role of carbon in the negative plate of advanced lead–carbon batteries, *ECS Trans.* 41 (13) (2012) 45–69.
- [32] H. Yanga, Y. Qiu, X. Guo, Effects of PPy, GO and PPy/GO composites on the negative plate and on the high-rate partial-state-of-charge performance of lead–acid batteries, *Electrochim. Acta* 215 (2016) 346–356.
- [33] P. Atanassova, A. DuPasquier, M. Oljaca, P. Nikolov, M. Matrakova, D. Pavlov, Carbon additives for advanced lead–acid battery applications, 14th European Lead Battery Conference (2014).
- [34] L.T. Lam, H. Ceylan, N.P. Haigh, T. Lwin, D.A.J. Rand, Influence of residual elements in lead on oxygen- and hydrogen-gassing rates of lead–acid batteries, *J. Power Sources* 195 (2010) 4494–4512.
- [35] L.T. Lam, J. Furukawa, Improved Energy Storage Device, WO 2008/070914, PCT/AU2007/001916 19, June (2008).
- [36] B. Hong, L. Jiang, H. Xue, F. Liu, M. Jia, J. Li, Y. Liu, Characterization of nano-lead-doped active carbon and its application in lead–acid battery, *J. Power Sources* 270 (2014) 332–341.
- [37] M. Blecua, E. Fatas, P. Ocon, J. Valenciano, F. de la Fuente, F. Trinidad, Influences of carbon materials and lignosulfonates in the negative active-material of lead–acid batteries for microhybrid vehicles, *J. Energy Storage* 11 (2017) 55–63.
- [38] W. Tiedemann, J. Newman, Modelling of the charge-acceptance of lead–acid batteries, *J. Electrochem. Soc.* 122 (1975) 70–74.
- [39] H. Yang, Y. Qiu, X. Guo, Lead oxide/carbon black composites prepared with a new pyrolysis-pickling method and their effects on the high-rate partial-state-of-charge performance of lead–acid batteries, *Electrochim. Acta* 235 (2017) 409–421.
- [40] L. Wang, H. Zhang, W. Zhang, G. Cao, H. Zhao, Y. Yang, Enhancing cycle performance of lead–carbon battery anodes by lead-doped porous carbon composite and graphite additives, *Mater. Lett.* 206 (2017) 113–116.
- [41] L. Wang, H. Zhang, W. Zhang, H. Guo, G. Cao, H. Zhao, Y. Yang, A new nano lead-doped mesoporous carbon composite as negative electrode additives for ultralong-cyclability lead–carbon batteries, *Chem. Eng. J.* 337 (2018) 201–209.
- [42] J.R. Miller, Capacitors, in: J. Garche, C. Dyer, P.T. Moseley, Z. Ogumi, D.A.J. Rand, B. Scrosati (Eds.), *Encyclopedia of Electrochemical Power Sources*, Vol. 1 Elsevier, Amsterdam, The Netherlands, 2009, pp. 587–599 ISBN 978-0-444-52093-7.
- [43] V. Augustyn, P. Simon, B. Dunn, Pseudocapacitive oxide materials for high-rate electrochemical energy storage, *Energy Environ. Sci.* 7 (2014) 1597–1614.
- [44] Y.M. Volkovich, P.A. Shmatko, High energy density supercapacitor, Proceedings of the Eighth International Seminar on Double-Layer Capacitors and Similar Energy Storage Devices (1998).
- [45] E. Lust, G. Nurk, A. Janes, M. Arulepp, L. Permann, P. Nigu, P. Moller, Electrochemical properties of nanoporous carbon electrodes, *Condens. Matter Phys.* 5 (2002) 307–327.
- [46] J.-P. Randin, E. Yeager, Differential capacitance study on the basal plane of stress-annealed pyrolytic graphite, *J. Electroanal. Chem. Interfacial Electrochem.* 36 (1972) 257–276.
- [47] J.-P. Randin, E. Yeager, Differential capacitance study on the edge orientation of pyrolytic graphite and glassy carbon electrodes, *J. Electroanal. Chem. Interfacial Electrochem.* 58 (1975) 313–322.
- [48] A. Pandolfo, A.F. Hollenkamp, Carbon properties and their role in supercapacitors, *J. Power Sources* 157 (2006) 11–27.
- [49] J. Robertson, Electron affinity of carbon systems, *Diam. Relat. Mater.* 5 (1996) 797–801.
- [50] J. Xiang, C. Hu, L. Chen, D. Zhang, P. Ding, D. Chen, H. Liu, J. Chen, X. Wu, X. Lai, Enhanced performance of Zn(II)-doped lead–acid batteries with electrochemical active carbon in negative mass, *J. Power Sources* 328 (2016) 8–14.
- [51] A. Aleksandrova, M. Matrakova, St. Ruevski, P. Nokolov, D. Pavlov, Effect of Novel ZnO Additive on the Performance of Lead–acid Battery Negative Electrode, LABAT' 2017, Golden Sands Resort, Bulgaria, 2017 13–16 June.
- [52] Y. Jiang, H. Zhu, C. Yu, X. Cao, L. Cheng, R. Li, S. Yang, C. Dai, Effects of carbon additives on the HRPSoC performance of lead carbon batteries and their low temperature performance, *Int. J. Electrochem. Sci.* 12 (2017) 10882–10893.
- [53] P.T. Moseley, R.F. Nelson, A.F. Hollenkamp, The role of carbon in valve-regulated lead–acid battery technology, *J. Power Sources* 157 (2006) 3–10.
- [54] K. Takai, M. Oga, H. Sato, T. Enoki, Y. Ohki, A. Taomoto, K. Suenaga, S. Iijima, Structure and electronic properties of a non-graphitic disordered carbon system and its heat-treatment effects, *Phys. Rev. B* 67 (2003) 214202-1–214202-11.
- [55] K. Kinoshita, K. Zaghib, Negative electrodes for Li-ion batteries, *J. Power Sources* 110 (2002) 416–423.
- [56] T. Enoki, M. Suzuki, M. Endo, *Graphite Intercalation Compounds and Applications*, Oxford University Press, Oxford, UK, 2003 ISBN: 9780195128277.
- [57] P. Schaffautl, *Journal für praktische Chemie* 21 (1841) 155.
- [58] G.A. Saunders, Electron transport in graphites and carbons, in: L.C.F. Blackman (Ed.), *Modern Aspects of Graphite Technology*, Academic Press, London/New York, 1970, pp. 79–127.
- [59] S. Basu, C. Zeller, P. Flanders, C.D. Fuerst, W.D. Johnson, J.E. Fischer, Synthesis and properties of lithium-graphite intercalation compounds, *Mater. Sci. Eng.* 38 (1979) 275–283.
- [60] Y. Maeda, Y. Okemoto, M. Inagaki, Electrochemical formation of graphite-sulfuric acid intercalation compounds on carbon fibers, *J. Electrochem. Soc.* 132 (1985) 2369–2372.
- [61] N. Iwoshita, H. Shioyama, M. Inagaki, Potential change during intercalation of sulfuric acid in host carbons with different textures, *Synth. Met.* 73 (1995) 33–40.
- [62] F. Kang, T.-Y. Zhang, Y. Leng, Electrochemical synthesis of sulfate graphite intercalation compounds with different electrolyte concentrations, *J. Phys. Chem. Solids* 57 (1996) 883–888.
- [63] C. Nutzenadel, A. Züttel, D. Chartouni, L. Schlapbach, Electrochemical storage of hydrogen in nanotube materials, *Electrochem. Solid State Lett.* 2 (1999) 30–32.
- [64] A.K.M. Fazle Kibria, Y.H. Mo, K.S. Park, K.S. Nahm, M.H. Yun, Electrochemical hydrogen storage behaviors of CVD, AD and LA grown carbon nanotubes in KOH medium, *Int. J. Hydrogen Energy* 26 (2001) 823–829.
- [65] E. Frackowiak, F. Béguin, Electrochemical storage of energy in carbon nanotubes and nanostructured carbons, *Carbon* 40 (2002) 1775–1787.
- [66] P. Kurzweil, Electrochemical double-layer capacitors: carbon materials, in: J. Garche, C. Dyer, P.T. Moseley, Z. Ogumi, D.A.J. Rand, B. Scrosati (Eds.), *Encyclopedia of Electrochemical Power Sources*, Vol. 1 Elsevier, Amsterdam, The Netherlands, 2009, pp. 634–648 ISBN 978-0-444-52093-7.
- [67] H.P. Boehm, Some aspects of the surface chemistry of carbon blacks and other carbons, *Carbon* 32 (1994) 759–769.
- [68] D. Qu, H. Shi, Studies of activated carbons used in double-layer capacitors, *J. Power Sources* 74 (1998) 99–107.
- [69] S. Shiraishi, H. Kurihara, A. Oya, Preparation and electric double layer capacitance of mesoporous carbon, *Carbon Sci.* 1 (2001) 133–137.
- [70] M. Endo, Y.J. Kim, T. Takeda, T.H.T. Maeda, K. Koshiba, H. Hara, M.S. Dresselhaus, Poly(vinylidene chloride)-based carbon as an electrode material for high power capacitors with an aqueous electrolyte, *J. Electrochem. Soc.* 148 (2001) A1135–A1140.
- [71] S. Lowell, J.E. Shields, *Powder Surface-area and Porosity*, 3rd ed., Chapman & Hall, London, UK, 1991 ISBN 978-94-015-7955-1.
- [72] J. Kresh, A. Soffer, Double layer capacitance and charging rate of ultra-microporous carbon electrodes, *J. Electrochem. Soc.* 124 (1977) 1379–1385.
- [73] G. Salitra, A. Soffer, L. Eliad, Y. Cohen, D. Aurbach, Carbon electrodes for double-layer capacitors I. Relations between ion and pore dimensions, *J. Electrochem. Soc.* 147 (2000) 2486–2493.
- [74] B.E. Conway, *Electrochemical Supercapacitors: Scientific Fundamentals and Technological Applications*, Springer, USA, 1999 ISBN 978-1-4757-3058-6.
- [75] K. Kinoshita, X. Chu, *The Electrochemical Society, Proceedings of the Symposium on Electrochemical Capacitors*, Vol. 95–25, Pennington, NJ, USA, 1995, pp. 171–180.
- [76] C.A. Leon y Leon, L.R. Radovan, *Interfacial chemistry and electrochemistry of carbon surfaces, Chemistry and Physics of Carbon Vol. 24* Marcel Dekker, New York, USA, 1994, pp. 213–310.
- [77] D. Qu, Studies of the activated carbons used in double-layer supercapacitors, *J. Power Sources* 109 (2002) 403–411.
- [78] R.L. McCreery, K.K. Cline, Carbon electrodes, in: P.T. Kissinger, W.R. Heineman (Eds.), *Laboratory Techniques in Electroanalytical Chemistry*, 2nd ed., Marcel Dekker, New York, USA, 1996, pp. 293–332.
- [79] H. Tamai, K. Masayuki, M. Morita, H. Yasada, Highly mesoporous carbon electrodes for electric double-layer capacitors, *Electrochem. Solid State Lett.* 6 (2003) A214–A217.
- [80] A. Burke, M. Miller, Experiment Studies of Carbon Enhanced Lead–acid Cells: Pulse Tests and Related Mechanisms, Report C5 to Advanced Lead–Acid Battery Consortium (ALABC), Durham, NC, USA, December (2010).
- [81] D. Pavlov, T. Rogachev, P. Nikolov, Influence of expander components on the processes at the negative plates of lead–acid cells on high-rate partial-state-of-charge cycling: part I: effect of lignosulfonates and BaSO<sub>4</sub> on the processes of charge and discharge of negative plates, *J. Power Sources* 195 (2010) 4435–4443.
- [82] S. Trasatti, Work function, electronegativity, and electrochemical behaviour of metals: III. Electrolytic hydrogen evolution in acid solutions, *J. Electroanal. Chem. Interfacial Electrochem.* 39 (1972) 163–184.
- [83] Na Li, Xiaoliang Ma, Qingfang Zha, Kyungsoo Kim, Yongsheng Chen, Chunshan Song, *Carbon* 49 (2011) 5002–5013.
- [84] W. Cai, K. Qi, Z. Chen, X. Guo, Y. Qiu, Effect of graphene oxide with different oxygenated groups on the high-rate partial-state-of-charge performance of lead–acid batteries, *J. Energy Storage* 18 (2018) 414–420.